Third Quarterly Report

Development of Uniform and Predictable Battery Materials for Nickel-Cadmium Aerospace Cells

(8 November 1968 — 7 February 1969)

Contract No.: NAS5-11561

Prepared by

Tyco Laboratories, Inc.
Bear Hill
Waltham, Massachusetts 02154

for

Goddard Space Flight Center
Greenbelt, Maryland

Third Quarterly Report

Development of Uniform and Predictable Battery Materials for Nickel-Cadmium Aerospace Cells

(8 November 1968 — 7 February 1969

Contract No.: NAS5-11561

Goddard Space Flight Center

Contracting Officer: A. L. Essex

Technical Monitor: Gerald Halpert

Prepared by

Tyco Laboratories, Inc.
Bear Hill
Waltham, Massachusetts 02154

Project Manager: John M. Parry

for

Goddard Space Flight Center
Greenbelt, Maryland

ABSTRACT

This report describes studies of the loose or dry sintering of INCO types 255 and 287 carbonyl nickel powder. The objective of this period was to define the factors in the sintering process that are important in the preparation of uniform and reproducible plaques for nickel cadmium batteries. The program also set out to examine the influence on uniformity and reproducibility of variations in physical characteristics inherent in these fragile filamentary powders from batch to batch. Variations were deliberately introduced into our samples by blending the two types of powder. We were also interested in the blending process itself as a potential source of nonuniform plaque properties, since blending of various powder batches is a standard commercial practice to meet a particular bulk density specification.

Plaques were prepared by loose sintering in a graphite mold at a range of sintering times and sintering temperatures. The following physical measurements were made on the plaque: weight per unit area, thickness, porosity, BET surface area, pore size distribution, resistivity, and mechanical strength. By cutting the 6- by 4- by 0.030-in. nominal size plaques into nine pieces, we were able to assess uniformity. Reproducibility was tested with selected duplicate experiments.

The principal conclusions are as follows. There is little difference in behavior between the two powders: plaques of the same porosity (obtained, for example, by sintering the 255 powder for a longer time than the 287) show comparable surface area, mechanical strength, and conductivity. Since most of the shrinkage occurs in the first few minutes of sintering, it would be advisable from a uniformity point of view to use sintering times that correspond to the plateaus in the shrinkage curve, i.e., in excess of 30 min. The decrease in porosity of approximately 5% at these extended sintering times is small compared to the advantages gained in reproducibility. There is also a factor of three increase in conductivity. More conductive plaques will minimize any intrinsic inhomogeneity under high drain rate operation.

Though good reproducibility was obtained in the loose sintering process (thickness to ± 0.0003 in., porosity to $\pm 0.5\%$, surface area to $\pm 3\%$, etc.), uniformity was not good. Definite trends in physical properties across the plaques could be related to the leveling technique. Loose sintering is therefore not a practical method to obtain highly uniform plaques, but it does provide valuable information on the sintering characteristics of these powders.

The measurements of the physical characteristics of the blended powders and the plaques derived from them indicate that the blending process markedly affects the properties of the powder and, in addition, does not produce a homogeneous mixture. From this we conclude that blending is detrimental in a process to produce uniform plaques. Without blending, reproducibility must be obtained by controlled variation of the sintering conditions.

Apparent disagreement between pore size distributions obtained by quantitative metallography and by mercury porosimetry has been shown to be due to a misinterpretation of the porosimetry curves. The reproducible rapid increase in intruded volume is indicative of a breakthrough pressure rather than a sharp distribution of pore size.

Table of Contents

List of Illustrations

List of Illustrations (Cont.)

List of Tables

I. INTRODUCTION

This project seeks to specify the conditions under which reproducible and highly uniform nickel cadmium battery plates can be prepared.

Since all the major manufacturers currently use INCO carbonyl nickel powders for the preparation of the porous plaques to support the active materials for one or both electrodes of the nickel cadmium couple, the experimental work has initially centered on a study of these materials. In an earlier report we have described tests of the uniformity of the physical characteristics of several batches of INCO carbonyl nickel powders. This examination also included an assessment of the magnitude of sampling and experimental errors. Both the latter were found to be small (rms deviations $< 1\%$). The bulk density and surface area of the various batches of powders were, however, spread over a range of approximately 10% of the mean value. These variations are more likely to be a result of mechanical handling than of variations in the batch manufacturing process.

Extensive mechanical handling, particularly of larger samples (> 50 lb), can change the physical characteristics of a powder because the filament shaped particles are easily broken. This will be discussed in more detail in this report in a different context.

This report describes our study of the sintering characteristics of these powders and the effect of sintering variables on the properties of the plaque. Our experimental approach was based on a loose or gravity sintering process carried out in a controlled atmosphere (dry hydrogen) furnace with a very flat temperature profile. This method was chosen because of its relative simplicity and because, in the absence of a support screen (essential in other methods of plaque fabrication and for practical electrodes), it affords more straightforward observation of the sintering behavior of the nickel powders. A slurry coating process will, however, be used for the manufacture of plaques for the balance of the program, since this is the process used to produce aerospace plaques and, as will be discussed below, loose sintering does not result in very uniform material.

The work described here can be considered under three main headings: (1) the effect of sintering conditions on plaque characteristics for both type 255 and 287 powders, (2) uniformity and reproducibility tests, and (3) the effect of the physical characteristics of the powder (varied in a controlled manner by blending type 255 and 287 powders) on plaque properties. Some of the results presented here were described but not discussed in the previous report. The disagreement in values for the average pore size derived from quantitative metallography and mercury porosimetry data, also mentioned in the previous report, is explained in terms of the general physical characteristics of the plaque.

II. EXPERIMENTAL METHODS AND DATA: MOLD FILLING AND SINTERING

Plaques LN-14 through LN-29 were prepared by the loose sintering of either type 255 or 287 carbonyl powder in a graphite mold. The sintering conditions and the porosity and thickness of the plaques produced are listed in Table I. Plaques LN-1 to LN-14 were discussed in the previous report, and essentially represented our efforts to define experimental techniques. In this section we will list all the data in tabular form. The figures will be discussed with graphical presentations in the following section.

The procedure for mold filling was to sieve the powder through a 200-mesh screen into the mold, a 6- by 4- by 0.030-in. undercut in an 8- by 5- by 0.25-in. graphite block, followed by leveling with a steel straightedge (striking blade). The leveling technique that produced the most satisfactory plaques consisted of holding the edge parallel to the 4-in. side of the mold and moving it in a zig-zag pattern across the mold. This approach has the advantage that the excess powder is removed at the sides of the plaque and does not build up excessively in front of the striking blade. Because of the poor flow characteristics of the filamentary carbonyl powders, buildup in front of the blade causes compaction, tearing (cracking), or undercutting of the surface. In the event that any of these features did occur in practice, the whole process was restarted. Great care was taken in handling the molds at this stage, since jarring or vibration has an adverse effect on the distribution of the powder.

Each mold was introduced into the furnace under dry hydrogen. Typically, a temperature drop of 15 °C was observed, but the set temperature was recovered within 3 min. The temperature profile of the furnace showed less than a 3 °C variation over a 13-in. length. At the end of the sintering time, the mold was removed to the water jacketed region of the furnace, still under hydrogen, where the temperature dropped rapidly to ~150 °C.

Several mold designs were used. The initial stainless steel molds were found to warp. The graphite molds resulted in some sticking, but a

very light dusting with zirconia was effective in preventing this. The final design consisted of a graphite mold with a Vycor liner which avoided the sticking problem without the use of zirconia. For the data presented below on the influence of sintering conditions on plaque properties, the measurements were made with the graphite mold. The plaques prepared to test the influence of powder properties on plaque characteristics were made in the Vycor lined molds.

The plaques were characterized in terms of thickness, shrinkage, surface area, porosity and pore size distribution, resistivity, and mechanical strength.

Area and volume shrinkages (Table II) were calculated from the plaque and mold dimensions. The surface area was measured using the BET technique with krypton as the adsorbate (surface areas down to 500 cm^2 can be measured by this method). The results, presented in Table III, are expressed as m^2/g, and m^2/cm^3 of plaque. The first figure represents one of the best methods of assessing uniformity, since the weight of the sample is readily measured precisely. The m^2/cm^3 figure depends on measurement of the dimensions of relatively small samples and so is slightly less precise, but it does take into account variations in porosity and thickness. One may then assess the changes in morphology of the nickel powder as a function of sintering conditions. (This factor is important in impregnation.)

The average porosity of the plaques (see Table I) was determined from their weight and dimensions; pore size distribution was determined by mercury porosimetry using a commercially available porosimeter (Micromeritics model 900). The latter measurements give rise to pore sizes (based on a cylindrical pore model) that are significantly smaller than those obtained by quantitative metallography. This factor is discussed later.

Resistivity was measured using a four-point contact technique. This method ensures that errors due to contact resistance are avoided. Current is passed through the plaque from a pair of parallel indium contacts on opposite edges of the plaque; the resistivity is obtained by measuring the potential difference between two points a known distance apart and per-

pendicular to the indium contacts. The measurement is repeated at several points to ensure that the equipotential lines are parallel to the current carrying electrodes. The specific resistivities were calculated from Ohm's law knowing the current and the thickness of the plaque, and are presented in Table IV.

The determination of mechanical strength by a four-point bend test was described in detail in the Second Quarterly Report. The experimental results for the plaques prepared in this report period are presented in Table V. Uniformity and reproducibility tests carried out on plaques LN-26 and 27 are presented in Tables VI and VII. Each 6- by 4-in. plaque was cut into nine pieces. The letters in the tables refer to the following positions in the plaque:

A B C
D E F
G H I

The A B C edge was the 4-in. dimension. Resistivity and mechanical strength measurements are incomplete because of the limited quantities of material available.

The effect of the physical characteristics of the nickel powders on plaque properties was studied by blending type 255 and 287 powders. This approach to obtain variability in physical properties was considered to be preferable to studying several different nickel powders, since very few commercial powders meet the basic requirement of a low bulk density. Furthermore, the blending of carbonyl nickel powders to meet bulk density specifications is a standard commercial practice which may be detrimental from the standpoint of uniformity and reproducibility. The blending was carried out by placing the required weights of each powder in a large vessel containing a spiral of copper wire, and the jar was then rotated slowly (~5 rpm) for 30 min. The measurements presented here permit an examination of the effect of blending on uniformity.

The physical measurements made in the powder mixtures (M-1 20% 255, M-2 40% 255, etc.) are presented in Table VIII. The surface area was determined by the BET method using krypton; the bulk density was

was determined by the Scott Volumeter technique for non-freeflowing powders, the Fisher number using the Fisher subsieve sizer, and the average crystallite size by X-ray line broadening. Since the particle size distributions of the type 287 and 255 powders are not significantly different, it is not surprising that the distributions measured by sedimentation for M-2 and M-4 also show little difference.

The physical characteristics of plaques prepared from the powder mixtures by loose sintering in a Vycor lined graphite mold at 900 °C for 30 min. are given in Tables IX to XIII. Uniformity of porosity and thickness was assessed for all nine pieces of the plaque lettered A through J as described above. The surface area, resistivity, and mechanical strength were measured for sections B, E, and H of each plaque. Somewhat more complete measurements were made for plaques LN-32 and 33 prepared from powder M-2 in a check on reproducibility. These results are presented in Tables XIV and XV.

Table I. Plaque Preparation Conditions, Porosity, and Thickness

Plaque No., LN	Powder	Sintering Time, min	Sintering Temperature, °C	Porosity %	Thickness, in. x 10^3
18	255	15	800	88.2	23.5
16	255	30	800	87.5	25.3
19	255	60	800	87.5	25.8
22	255	15	900	87.5	23.8
14	255	30	900	83.7	22.0
23	255	60	900	84.3	22.6
20	287	15	800	86.9	24.0
17	287	30	800	82.9	26.0
21	287	60	800	83.5	24.5
24	287	15	900	84.5	25.0
15	287	30	900	77.9	24.8
25	287	60	900	79.3	23.8
26	287	30	800	See separate tables	
27	287	30	800		
28	287	30	800	83.4	24.3
29	255	10	800	89.0	25.2
	See text	20	800	89.0	25.2
		30	800	86.4	23.5

Table II. General Plaque Properties

Plaque No., LN	Weight, g	Area, cm^2	Volume, cm^3	Shrinkage to % Original Area*	Shrinkage to % Original Volume*
14	10.069	124.3	6.92	79.0	57.3
15	13.590	110.2	7.20	70.0	59.8
16	9.746	136.3	8.41	86.5	69.8
17	13.563	134.6	8.37	85.4	69.6
18	8.946	142.7	8.34	90.5	69.2
19	8.739	129.0	7.60	81.8	63.1
20	13.100	141.9	9.57	89.9	79.5
21	12.073	130.1	8.10	82.5	67.2
22	9.014	134.6	8.13	85.4	67.4
23	8.792	109.5	6.27	69.5	51.9
24	12.414	142.0	9.01	90.0	74.6
25	12.120	122.0	7.36	69.2	61.0
26	12.291	133.6	8.15	86.2	67.5
27	12.023	134.5	8.19	85.4	67.8
28	12.658	139.2	8.59	88.3	71.2
29	9.427	148.0	9.47	93.9	78.5
	9.426	145.0	9.30	92.0	77.0
	9.122	126.4	7.55	80.2	62.6

* Mold area = 157.8 cm^2, mold volume = 12.04 cm^3.

Table III. Surface Area as a Function of Plaque Preparation Conditions

Plaque No., LN	Powder	Sintering Time, min	Sintering Temperature, °C	Porosity, %	Surface Area m^2/g	Surface Area m^2/cm^3
18	255	15	800	88.2	0.198	0.208
16	255	30	800	87.5	0.168	0.187
19	255	60	800	87.5	0.186	0.263
22	255	15	900	87.5	0.167	0.185
14	255	30	900	83.7	0.151	0.217
23	255	60	900	84.3	0.140	0.196
20	287	15	800	86.9	0.163	0.181
17	287	30	800	82.9	0.151	0.230
21	287	60	800	83.5	0.130	0.194
24	287	15	900	84.5	0.159	0.219
15	287	30	900	77.9	0.127	0.250
25	287	60	900	79.3	0.111	0.204
26	287	30	800	See separate tables		
27	287	30	800			
28	287	30	800	83.4	—	
29	255	10	800	89.0	—	
		20	800	89.0	—	
		30	800	86.4	—	

Table IV. Resistivity as a Function of Plaque Preparation Conditions

Plaque No., LN	Powder	Sintering Time, min	Sintering Temperature, °C	Porosity, %	Resistivity, ohm-cm x 10^4
18	255	15	800	88.2	5.48
16	255	30	800	87.5	3.75
19	255	60	800	87.5	4.81
22	255	15	900	87.5	4.99
14	255	30	900	83.7	2.70
23	255	60	900	84.3	2.30
20	287	15	800	86.9	4.49
17	287	30	800	82.9	2.50
21	287	60	800	83.5	3.25
24	287	15	900	84.5	3.98
15	287	30	900	77.9	1.61
25	287	60	900	79.3	2.24
26	287	30	800	See separate tables	
27	287	30	800		
28	287	30	800	83.4	—
29	255	10	800	89.0	—
		20	800	89.0	—
		30	800	86.4	—

Table V. Mechanical Strength as a Function of Plaque Preparation Conditions

Plaque No., LN	Powder	Sintering Time, min	Sintering Temperature, °C	Porosity, %	Mechanical Strength, kg/cm^2
18	255	15	800	88.2	17.0
16	255	30	800	87.5	24.9
19	255	60	800	87.5	34.8
22	255	15	900	87.5	26.4
14	255	30	900	83.7	48.3
23	255	60	900	84.3	50.3
20	287	15	800	86.9	22.0
17	287	30	800	82.9	42.2
21	287	60	800	83.5	42.0
24	287	15	900	84.5	37.5
15	287	30	900	77.9	58.3
25	287	60	900	79.3	67.7
26	287	30	800	See separate tables	
27	287	30	800		
28	287	30	800	83.4	
29	255	10	800	89.0	
		20	800	89.0	
		30	800	86.4	

Table VI. Physical Characteristics of Plaque LN-26

Sample No.	Thickness, in.	Density, g/cm^3	Porosity, %	BET Surface Area			Mechanical Strength, kg/cm^2
				m^2/g	cm^2/cm^2	m^2/cm^3	
A	0.0243	1.541	82.70	0.147	139	0.227	
B	0.0228	1.591	82.10	0.122	112	0.194	39.56
C	0.0241	1.557	82.52	0.150	143	0.234	
D	0.0244	1.506	83.08	0.145	135	0.218	36.31
E	0.0238	1.527	82.85	0.157	148	0.240	
F	0.0240	1.558	82.51	0.145	138	0.226	
G	0.0247	1.492	83.23	0.156	147	0.233	
H	0.0242	1.403	84.19	0.141	122	0.198	33.31
I	0.0246	1.484	83.32	0.131	125	0.194	
Average	0.0241	1.518	82.95	0.144	134	0.217	

Table VII. Physical Characteristics of Plaque LN-27

Sample No.	Thickness, in.	Density, g/cm^3	Porosity, %	BET Surface Area m^2/g	BET Surface Area cm^2/cm^2	BET Surface Area m^2/cm^3	Mechanical Strength, kg/cm^2	Resistivity, ohm - cm x 10^4
A	0.0237	1.541	82.71	0.144	134	0.222		
B	0.0227	1.479	83.41	0.119	102	0.176	40.93	
C	0.0240	1.415	84.12	0.152	131	0.215		3.15
D	0.0238	1.569	82.63	0.152	144	0.238	48.90	3.15
E	0.0235	1.547	82.67	0.132	122	0.204		
F	0.0245	1.485	83.34	0.142	131	0.211		3.26
G	0.0246	1.584	82.28	0.141	139	0.223		
H	0.0241	1.503	83.11	0.147	135	0.221	35.40	
I	0.0245	1.467	83.54	0.135	127	0.198		
Average	0.0239	1.510	83.21	0.141	129	0.212		

Table VIII. Physical Characteristics of Blended Powders

	Powder	Surface Area, m^2/g	Bulk Density, g/cm^3	Fisher No., μ	Average Crystallite Size, Å
M-0	287	0.447	0.954	3.35	424
M-1	80% 287, 20% 255	0.460	0.915	3.29	422
M-2	60% 287, 40% 255	0.495	0.884	3.18	425
M-3	40% 287, 60% 255	0.518	0.823	3.12	393
M-4	20% 287, 80% 255	0.510	0.765	3.06	377
M-5	255	0.517	0.630	2.87	384

Table IX. Plaques From Blended Powders —— Uniformity of Porosity

	Powder Plaque No.					
Section*	M-0 LN-40	M-1 LN-38	M-2 LN-41	M-3 LN-42	M-4 LN-36	M-5 LN-39
A	82.9	85.0	83.5	84.9	85.1	89.0
B	82.6	84.5	83.4	85.1	86.1	88.6
C	82.7	84.7	82.9	85.3	85.6	88.8
D	83.1	84.6	83.3	85.7	85.2	88.8
E	82.7	84.7	83.1	84.9	86.2	88.4
F	82.9	84.7	82.8	85.3	86.1	88.4
G	82.4	86.7	83.7	84.9	85.3	89.0
H	83.6	85.1	83.8	85.3	85.5	89.1
I	85.4	84.3	82.5	85.2	85.7	88.9
Average	83.1	84.9	83.2	85.2	85.6	88.8

* A B C is the top edge of the mold, G H I the bottom.

Table X. Plaques From Blended Powders —— Uniformity of Thickness, in. x 10^3

	Powder Plaque No.					
	M-0	M-1	M-2	M-3	M-4	M-5
Section*	LN-40	LN-38	LN-41	LN-42	LN-36	LN-39
A	21.8	23.1	20.6	21.0	23.1	21.8
B	21.7	22.5	21.2	22.0	23.1	21.8
C	22.6	23.0	22.5	22.9	22.2	21.9
D	22.0	23.3	20.0	21.5	21.8	21.8
E	22.8	23.3	20.6	22.0	21.4	21.8
F	23.1	23.1	21.3	23.3	22.6	23.1
G	22.7	24.0	20.3	20.3	21.8	20.2
H	22.6	23.2	20.6	20.8	22.1	20.2
I	23.4	23.6	21.6	21.8	22.6	20.2

* A B C is the top edge of the mold, G H I the bottom edge.

Table XI. Plaques From Blended Powders —— Surface Area, m^2/g

Powder	Plaque No.	Section B	Section E	Section H
M-0	LN-40	0.123	0.139	0.131
M-1	LN-38	0.152	0.165	0.152
M-2	LN-41	0.142	0.168	0.139
M-3	LN-42	0.135	0.138	0.144
M-4	LN-36	0.151	0.152	0.144
M-5	LN-39	0.151	0.162	0.169
		m^2/cm^3		
M-0	LN-40	0.190	0.214	0.191
M-1	LN-38	0.209	0.224	0.201
M-2	LN-41	0.209	0.252	0.200
M-3	LN-42	0.179	0.186	0.188
M-4	LN-36	0.187	0.187	0.186
M-5	LN-39	0.153	0.186	0.164

Table XII. Plaques From Blended Powders —— Resistivity, ohm-cm x 10^4

Powder	Plaque No.	Section B	Section E	Section H
M-0	LN-40	25.6	24.3	25.3
M-1	LN-38	31.9	35.6	37.1
M-2	LN-41	25.5	25.7	26.1
M-3	LN-42	32.4	31.4	32.2
M-4	LN-36	28.5	33.4	35.0
M-5	LN-39	53.9	48.0	——

Table XIII. Plaques From Blended Powders —— Mechanical Strength, kg/ cm^2

Power	Plaque No.	Section B	Section E	Section H
M-0	LN-40	53.7	53.7	43.3
M-1	LN-38	36.4	36.8	29.4
M-2	LN-41	44.6	40.7	37.3
M-3	LN-42	33.7	38.0	39.0
M-4	LN-36	27.6	25.3	31.3
M-5	LN-39	18.8	18.8	14.3

Table XIV. Physical Characteristics of Plaque LN-32

Sample No.	Thickness, in. x 10^3	Density, g/cm^3	Porosity, %	BET Surface Area m^2/g	BET Surface Area cm^2/cm^2	BET Surface Area m^2/cm^3	Mechanical Strength, kg/cm^2
A	24.9	1.367	84.6	0.134	115	0.183	
B	25.0	1.511	83.0	0.126	122	0.190	43.02
C	25.6	1.359	84.7	0.112	99	0.152	59.53
D	24.7	1.473	83.4	0.131	121	0.193	
E	24.5	1.466	83.5	0.120	113	0.176	45.68
F	25.3	1.555	82.5	0.117	115	0.182	
G	23.4	1.531	82.8	0.122	110	0.187	
H	23.3	1.586	82.2	0.124	117	0.197	63.12
I	23.2	1.675	81.1	0.131	130	0.219	66.61
Average	24.4	1.503	83.1	0.124	116	0.187	

Table XV. Physical Characteristics of Plaque LN-33

Sample No.	Thickness, in. x 10^3	Density, g/cm^3	Porosity, %	BET Surface Area m^2/g	BET Surface Area cm^2/cm^2	BET Surface Area m^2/cm^3	Mechanical Strength, kg/cm^2	Resistivity, ohm-cm x 10^4
A	23.5	1.503	83.1	0.136	122	0.204		
B	23.8	1.491	83.2	0.109	98	0.163	57.71	
C	24.9	1.514	83.0	0.118	113	0.179	62.92	
D	24.8	1.565	82.4	0.119	126	0.186		2.44
E	24.2	1.505	83.1	0.131	122	0.197	50.42	2.46
F	23.1	1.516	83.0	0.127	114	0.192		2.36
G	21.5	1.625	81.7	0.118	104	0.192		2.08
H	22.0	1.605	81.9	0.124	111	0.199	62.02	2.15
I	22.6	1.636	81.6	0.111	104	0.182	78.45	1.96
Average	23.4	1.551	82.6	0.121	113	0.192		

III. DISCUSSION

A. General Plaque Properties as a Function of Sintering Conditions

Many of the features observed in the loose sintering of carbonyl nickel powders are exactly as one would expect (these will be discussed briefly for completeness). Others confirm relationships that might be expected to hold, while a few are difficult to explain.

Among the expected results is the decrease in porosity with increased sintering time and increased sintering temperature. These relationships are presented for type 255 and 287 powders in Figs. 1 to 3. * Under the same conditions, plaques prepared from the 255 powder have a higher porosity. Despite the high porosities (ranging from 80 to 90%), and the lack of a support screen, the 6- by 4- by 0.020-in. plaques are mechanically sound with a smooth hard surface. They may be held at one corner or flexed between the fingers without risk of damage.

An unusual feature of the results of Fig. 3 is that a higher porosity is observed for the plaques sintered for 60 min as opposed to those at 30 min. This is a result of the method of calculation of the porosity based on the weight and major dimensions of the plaque and the fact that the plaques sintered for 60 min are in all cases lighter than those sintered for 30 min. The consistency of the weights in Table XVI for both powders at both temperatures as a function of sintering time indicates that the starting quantities of powder did not show significant variation. Also, the shrinkage curves (Figs. 4 through 7) demonstrate that no major changes in dimension occur after the first few minutes of sintering. We must therefore conclude that there is an actual loss of material at extended sintering times.

A more detailed examination of the weight figures as a function of sintering time shows another unexpected feature. For each powder at each temperature examined, it would appear that there is an increase in weight between 15 and 30 min followed by the larger loss in weight between 30 and

*Note. These and other data are presented graphically for convenience only. No quantitative significance is attached to the lines drawn, since few points were determined and the scales in most cases are large relative to the accuracy of the measurements.

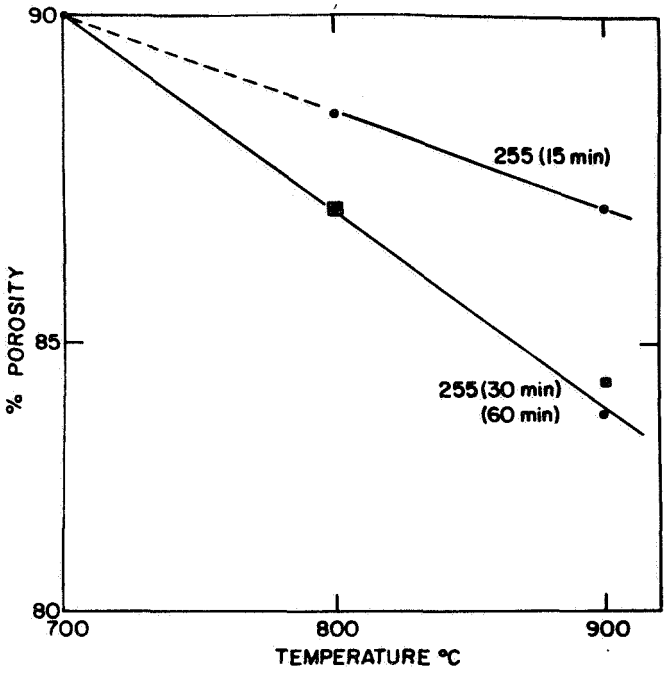

Fig. 1. Porosity versus sintering temperature, 255

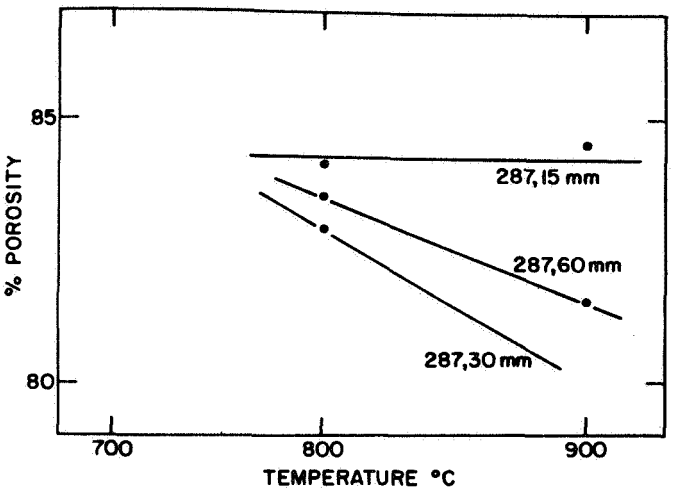

Fig. 2. Porosity versus sintering temperature, 287

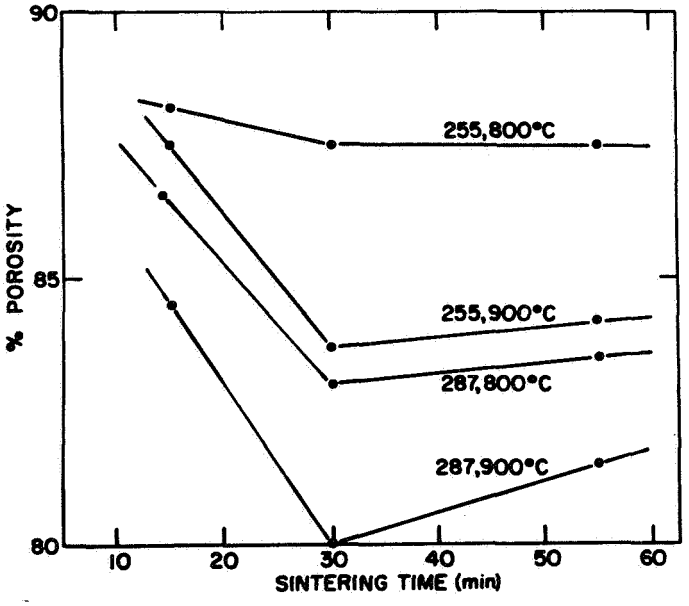

Fig. 3. Porosity versus sintering time

Table XVI. Variation of Plaque Weights

Powder	Sintering Conditions: Temperature, °C	Sintering Conditions: Time, min	Plaque No.	Weight, g
255	800	15	LN-18	8.946
		30	LN-16	9.746
		60	LN-19	8.739
	900	15	LN-22	9.014
		30	LN-14	10.069
		60	LN-33	8.792
287	800	15	LN-20	13.100
		30	LN-17	13.563
		60	LN-21	12.073
	900	15	LN-24	12.414
		30	LN-15	13.590
		60	LN-25	12.120

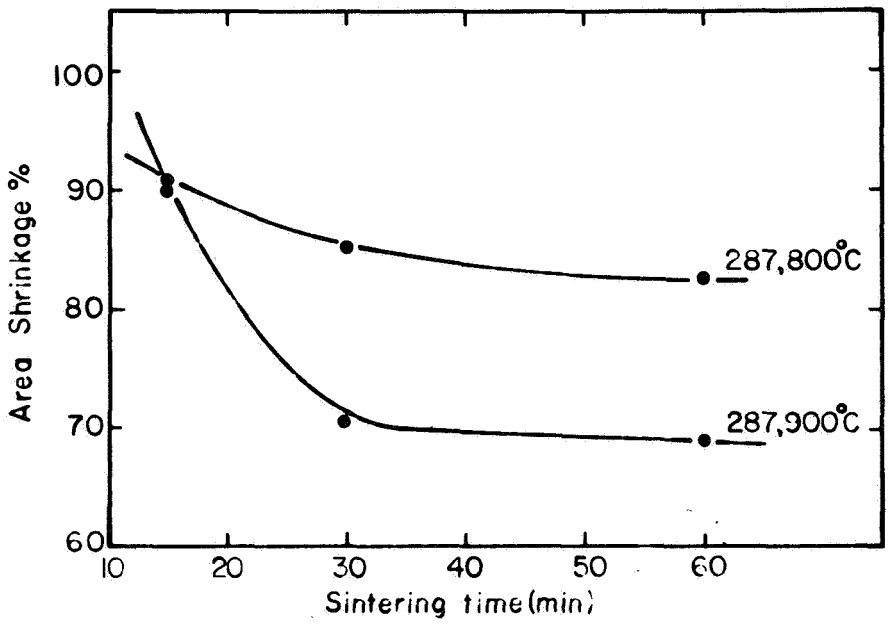

Fig. 4. Geometric area shrinkage versus sintering time, 287

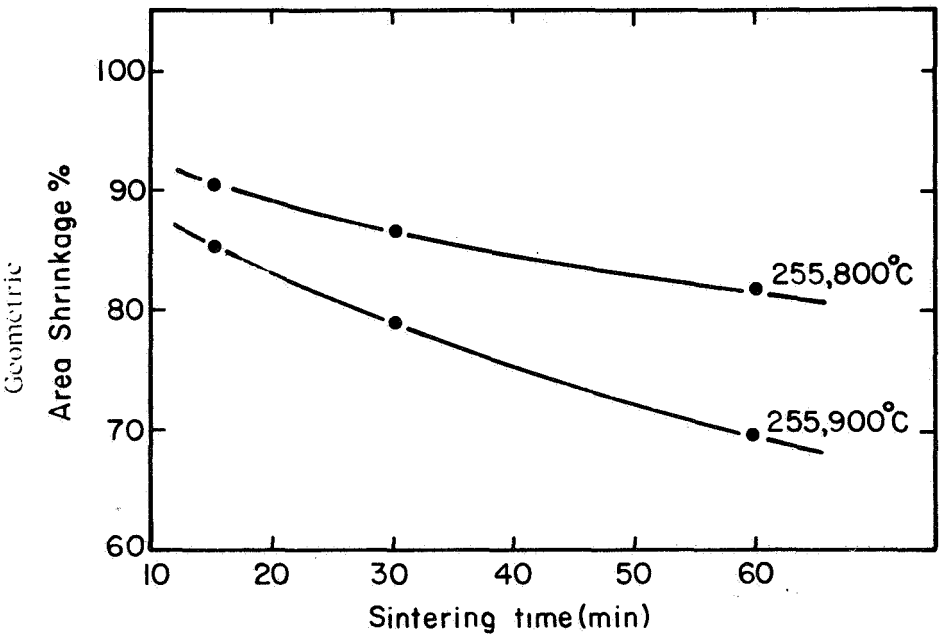

Fig. 5. Geometric area shrinkage versus sintering time, 255

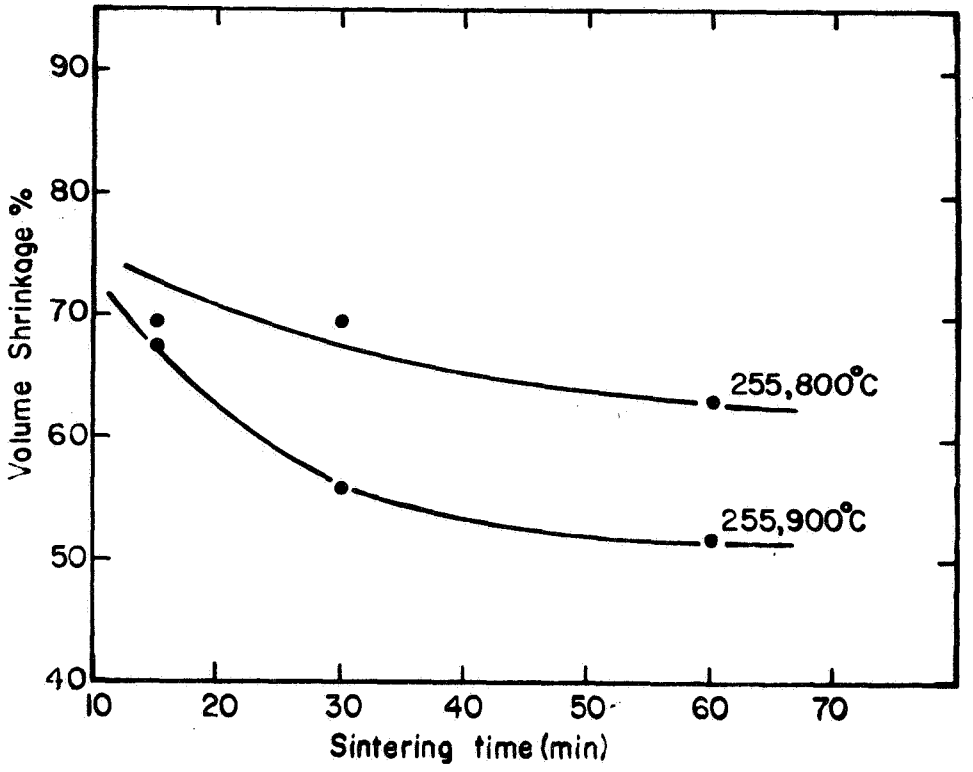

Fig. 6. Volume shrinkage versus sintering time, 255

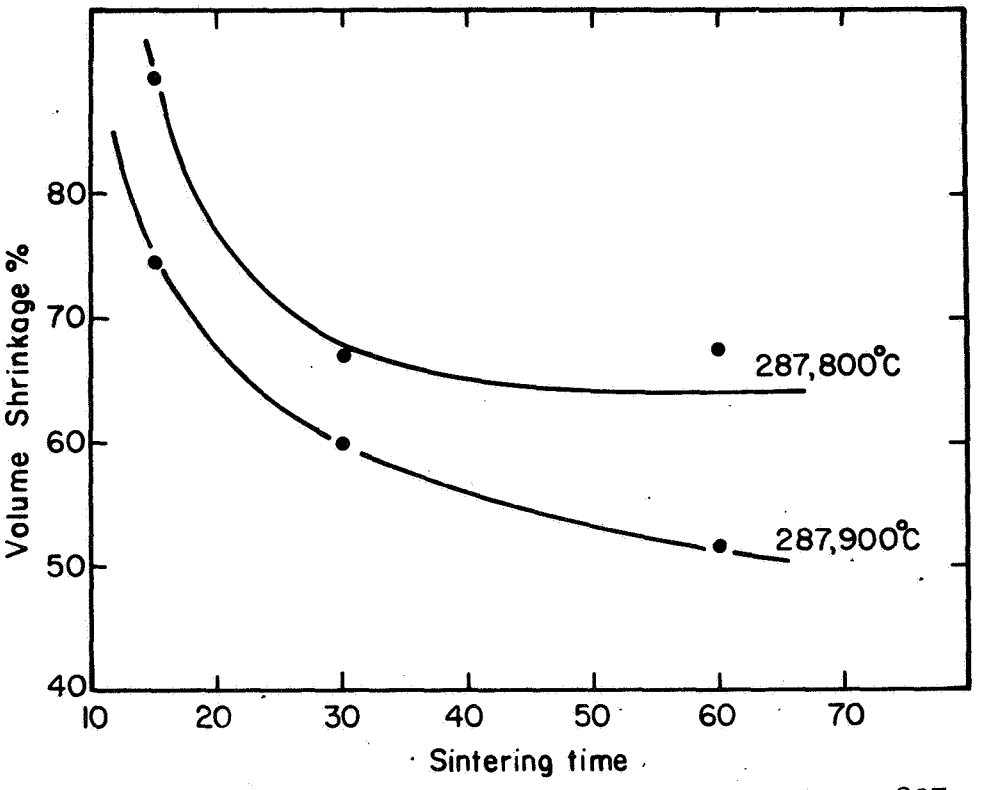

Fig. 7. Volume shrinkage versus sintering time, 287

60 min described above. No straightforward explanation can be offered for this behavior. It should be noted that the percentage of weight change (~ 5%) far exceeds changes that could be attributed to volatile impurities. However, it is possible that this behavior can be accounted for by a furnace defect. In these experiments, the relay restricting the nitrogen flow during automatic operation on hydrogen was chattering. There is then the possibility of introducing nitrogen into the hydrogen stream. At the time, this was not considered to be important but, since no effort is made to remove trace oxygen from the nitrogen (deoxo units and molecular sieves are used in the hydrogen line), some oxidation could have occurred. This could result in an initial increase in weight due to oxide formation followed by flaking or some other physical loss mechanism resulting in a decrease in weight. The relay has now been replaced and we will be repeating these measurements. Similar apparently inconsistent behavior is observed in the resistivity and specific surface area figures as a function of sintering times presented below.

As mentioned above, it is apparent from the shrinkage curves that most of the shrinkage occurs in the first few minutes. There are, however, indications that this process might be slower for the 287 powder (see, for example, the relatively steep regions of the curves in Fig. 7). The 255 curves show only a gradual increase in shrinkage with sintering time. The total shrinkage increases with temperature: the maximum geometrical area shrinkage is to approximately 70% of the original size for both types of powder; the maximum volume shrinkage is close to 50% for both powders.

The behavior of these powders on sintering, together with a knowledge of their morphology, enable us to develop a picture of the sintering process. Both types of powders have filamentary particles up to 20 μ or more in length with a spiky surface (these factors have been examined in detail in previous reports). The principal difference between the two powders is in filament diameter, with an average of approximately 3 μ for the 255 and approximately 1 μ for the 287. (The difference in cross-sectional area of the filaments readily accounts for the difference in the bulk densities of the two powders.)

On raising the temperature of the powder mass, the surface structure is rapidly destroyed which allows the powders to "settle" or pack down. For a sufficiently large increase in temperature, sintering begins so that the structure and thus the porosity is maintained. For extended sintering times (say, more than 5 min), further shrinkage occurs, but this is much smaller in magnitude and is a result of bulk and surface diffusion of nickel into the regions of surface contact (so called neck growth). The driving force for this process is the minimization of the surface energy, but since the diffusion rates are quite low and strongly temperature dependent, significant neck growth is not achieved without long sintering times at the higher sintering temperatures. It is unlikely that evaporation and condensation mechanisms contribute to neck growth at the commonly used sintering temperatures.

The extent of neck growth is reflected in an increase in mechanical strength and conductivity and a decrease in porosity. An example of the correlation between resistivity and shrinkage is given in Fig. 8. As will be discussed below, the loss in porosity is small (a few percent) compared to the improvements in mechanical strength and conductivity.

The variation of surface area in m^2/g as a function of sintering conditions is shown in Fig. 9. The plotted points at 60 min, particularly the 255, 800 °C point, are probably misleading because of the weight loss that occurs. If, as was suggested earlier, the weight loss was the result of flaking off of a surface oxide, then the m^2/g figure would be expected to increase. This factor is avoided if we examine instead the m^2/cm^3 figure which is not sensitive to weight changes. These results are presented in Fig. 10. The curve for the 255 powder at 800 °C is completely different from the other three, which show a maximum at 30 min. If we accept that the 255, 800 °C curve is anomalous, the pattern of the other curves is consistent with the formation of an oxide film of a greater surface roughness which is lost mechanically at longer times.

The effect of sintering temperature on surface area shown in Figs. 11 and 12 is as expected and is relatively small. The odd value obtained with the 255 powder at 800 °C for 60 min explains the unusual slope of the 60-min line in Fig. 11.

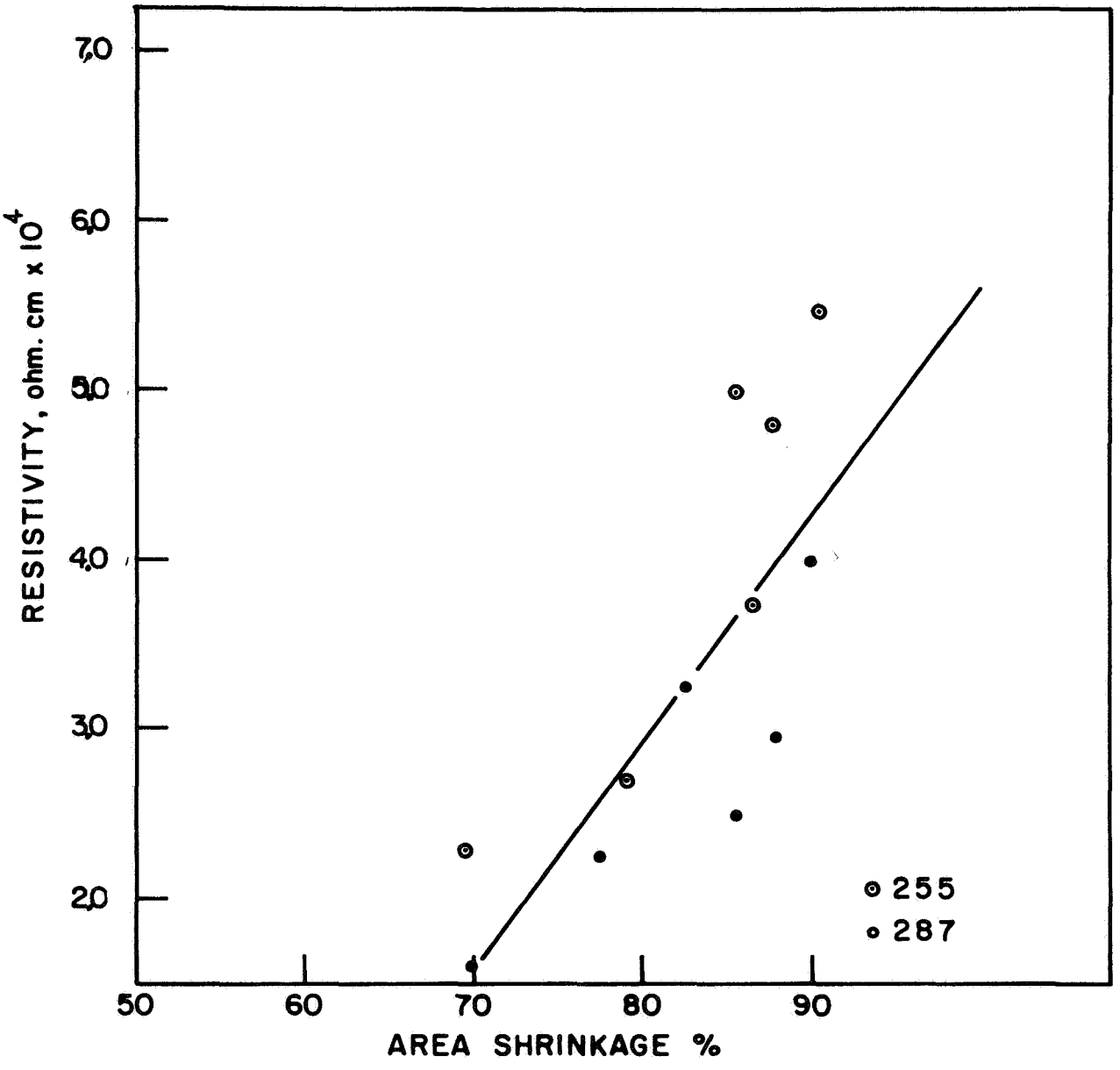

Fig. 8. Resistivity versus area shrinkage

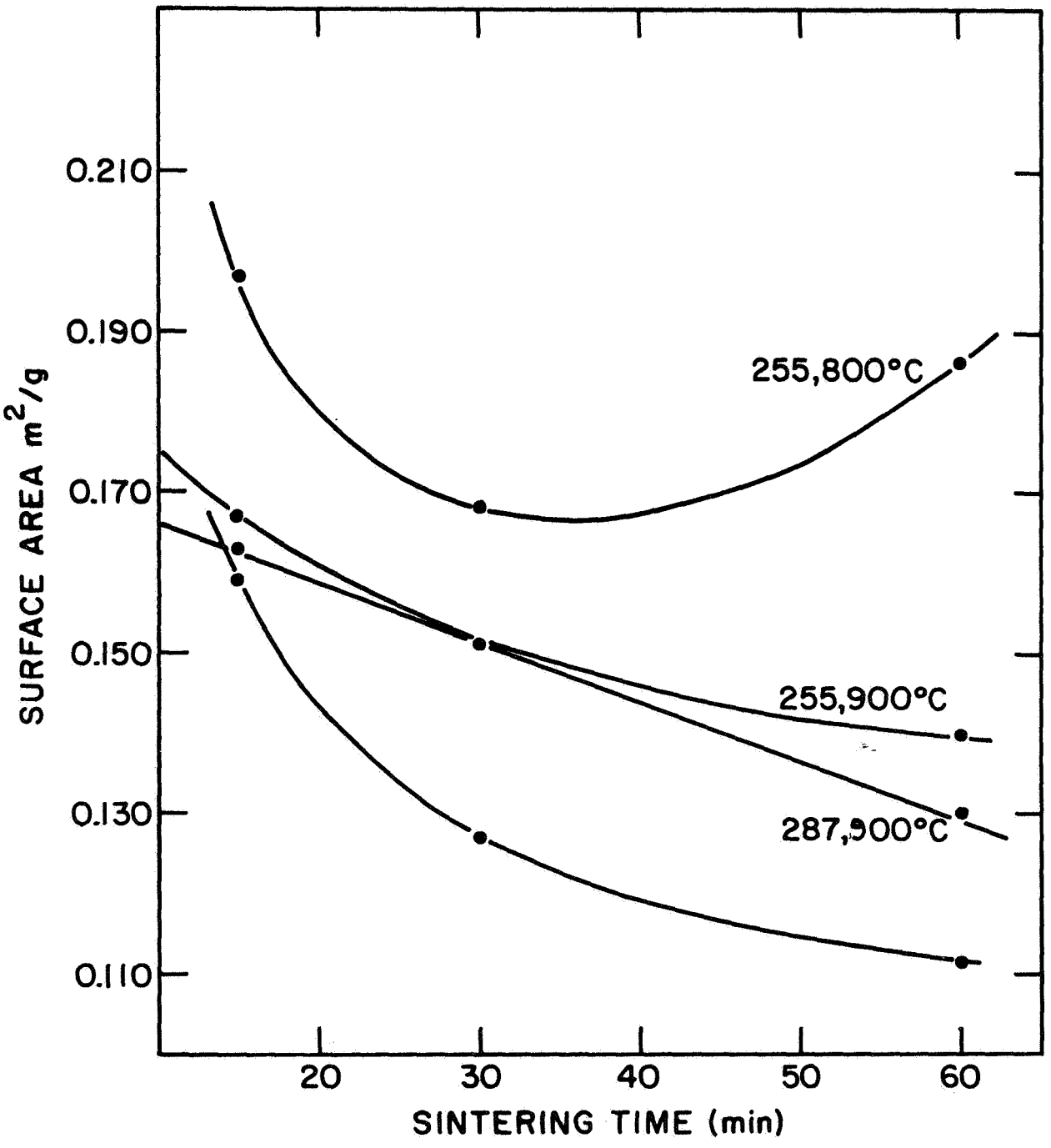

Fig. 9. Surface area versus sintering time

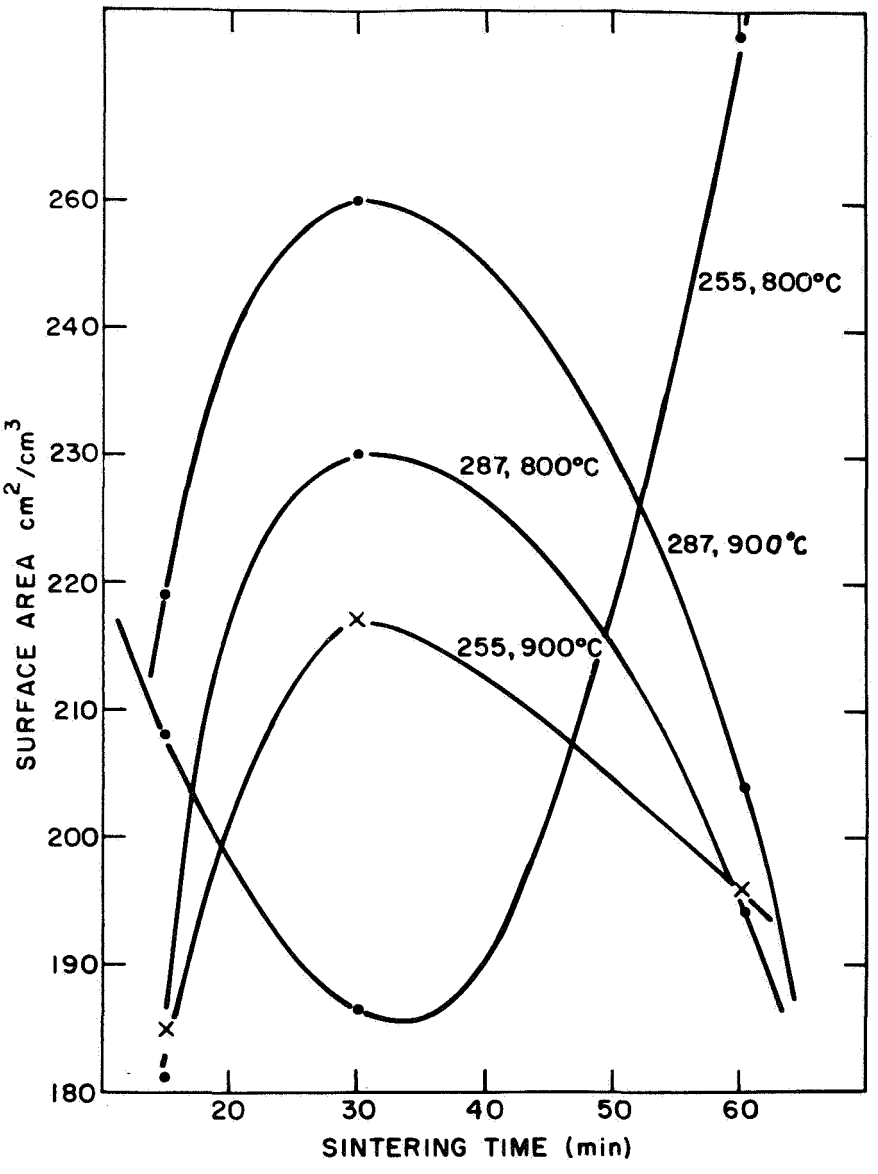

Fig. 10. Plaque surface area versus sintering time

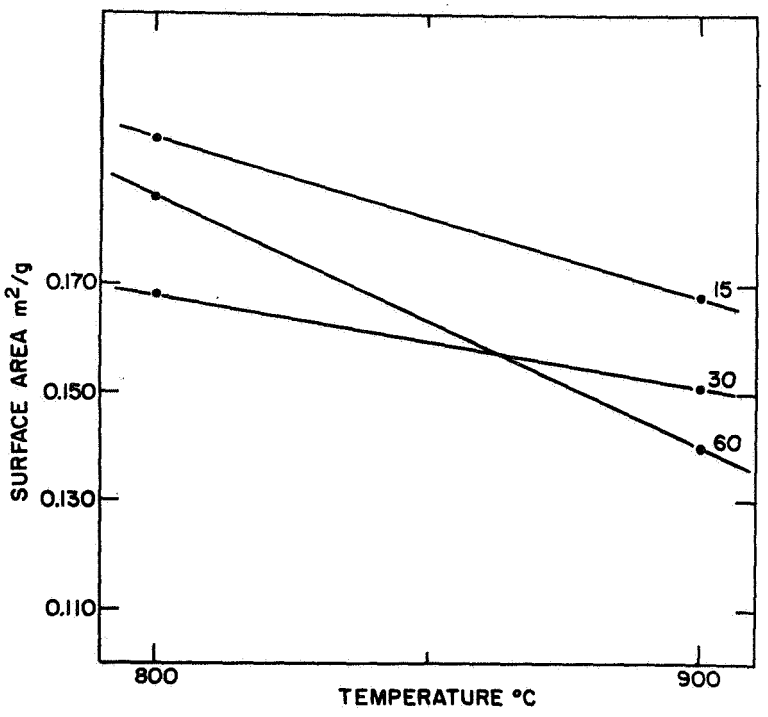

Fig. 11. Surface area versus temperature, 255

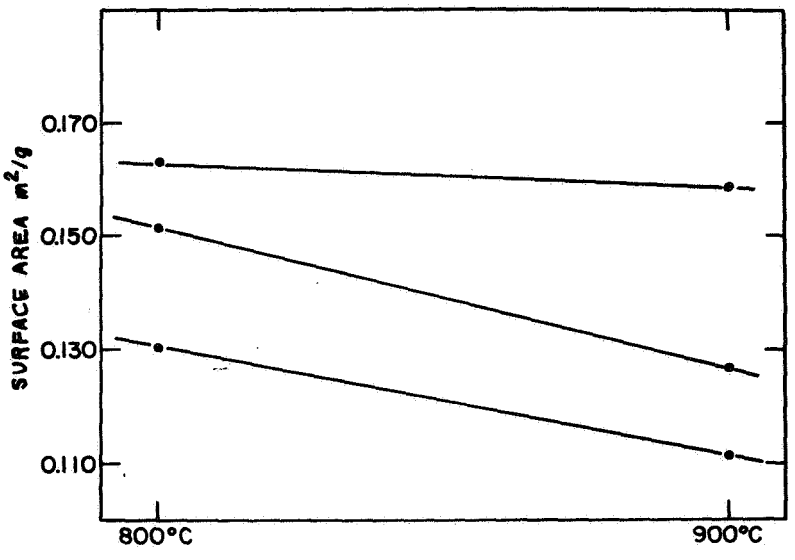

Fig. 12. Surface area versus temperature, 287

The variation in resistivity as a function of sintering time, shown in Figs. 13 and 14, is also anomalous. Three of the four curves show a minimum value at 30 min, the fourth (255 at 900 °C) shows approximately equal values at 30 and 60 min. This behavior is consistent with the weight loss observed, particularly if the explanation of a loss of material is accepted, and that this loss takes place uniformly over the surface. This would mean a marked effect in the neck region and an increase in resistivity.

The mechanical strength as a function of sintering temperature is shown in Fig. 15. The trend is for a relatively large increase in mechanical strength to occur between 15 and 30 min, but with only a small, if any, increase beyond that. Without a loss of material, the mechanical strength would be expected to increase continuously.

The interrelation of the physical properties of the plaques presents a more rational picture and encourages confidence in the experimental data, i.e., the effects discussed above are real and not a result of experimental inconsistencies.

Good linear relationships are obtained between porosity and shrinkage (see Figs. 16 and 17). This is an obvious result, but it enables us to plot the remainder of the results as a function of porosity only and still draw conclusions with respect to shrinkage.

For example, in Fig. 18, the pattern of change of resistivity with porosity is presented. The points are adequately represented by a single straight line, i.e., there is a random distribution of the results for the two types of powder. From this we may conclude that shrinkage is essential to the development of good conductivity. From a uniformity point of view, it might initially be considered that shrinkage should be inhibited since it is likely to occur in a nonuniform manner. However, it is probably more important for a large initial shrinkage to occur, since this will promote more particle to particle contact. Each of these contacts will be developed at the same rate by neck growth during the remainder of the sintering process. Thus, it is probably of greater practical significance to produce the marked decrease in resistivity associated with the more severe sintering conditions. For example, a decrease in resistivity by a factor of ~ 3 is obtained for only a 5%

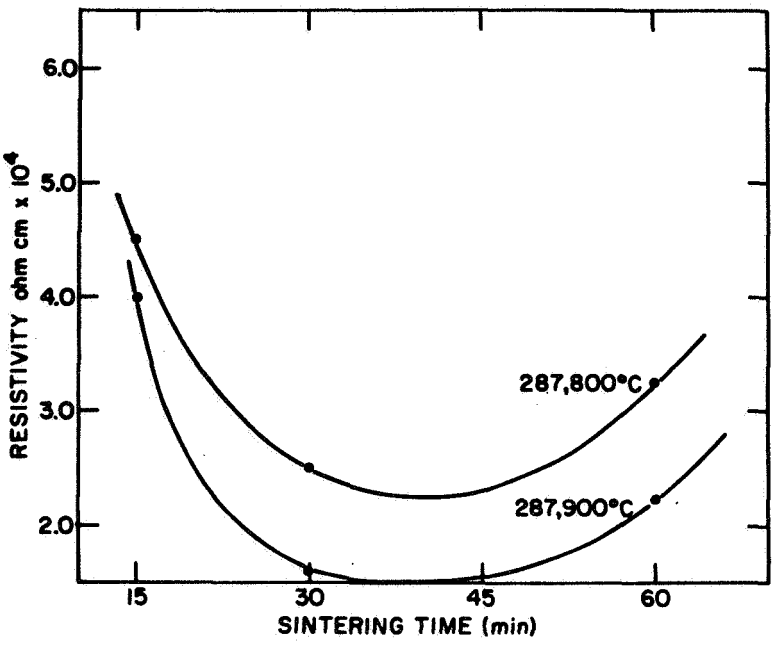

Fig. 13. Resistivity versus sintering time, 287

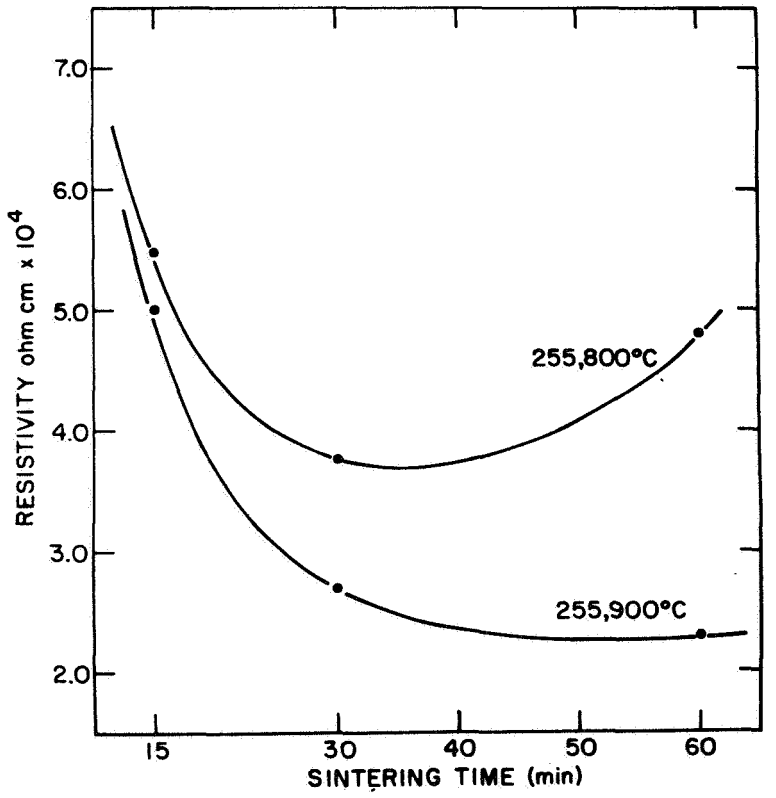

Fig. 14. Resistivity versus sintering time, 255

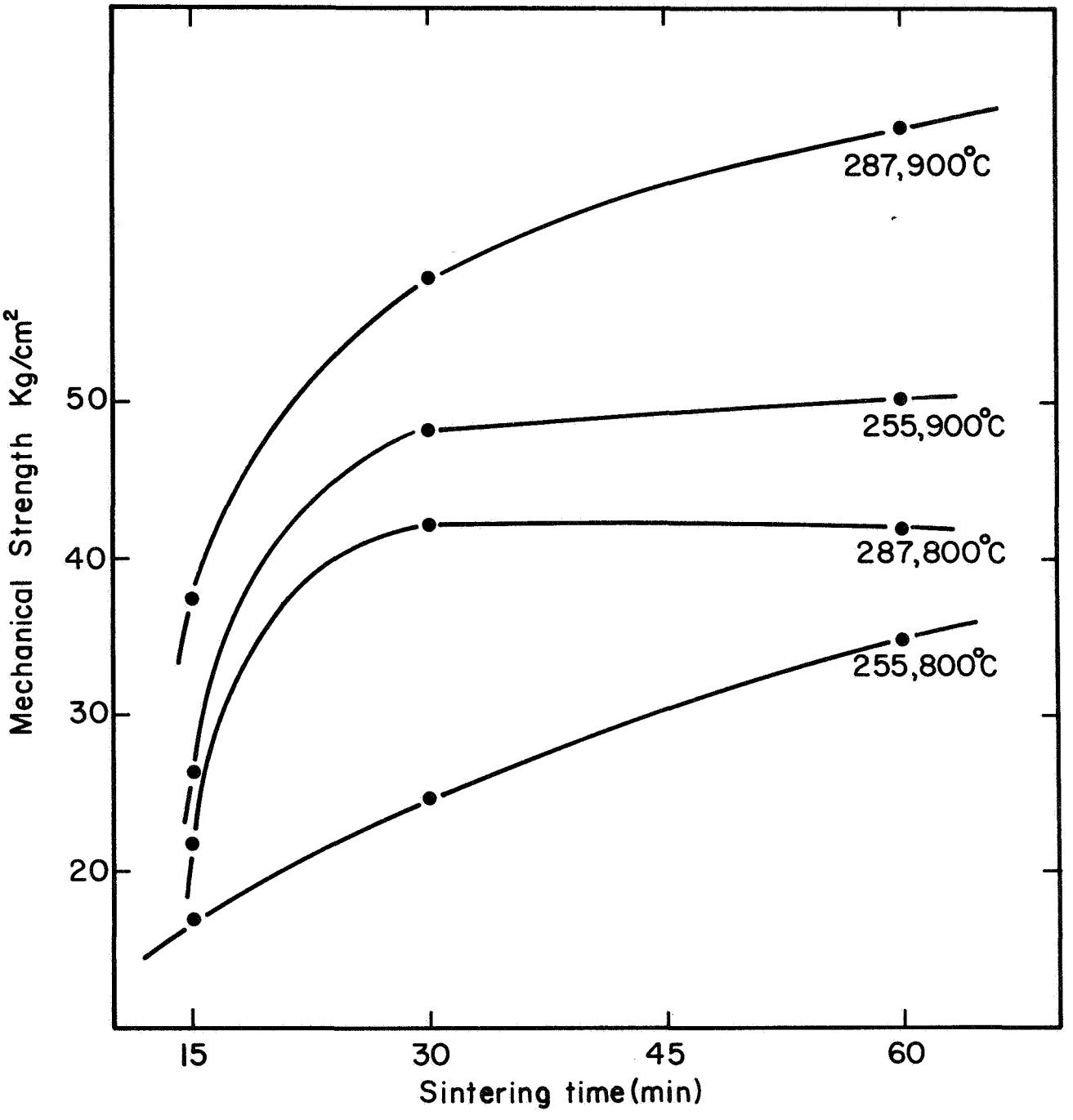

Fig. 15. Mechanical strength versus sintering time

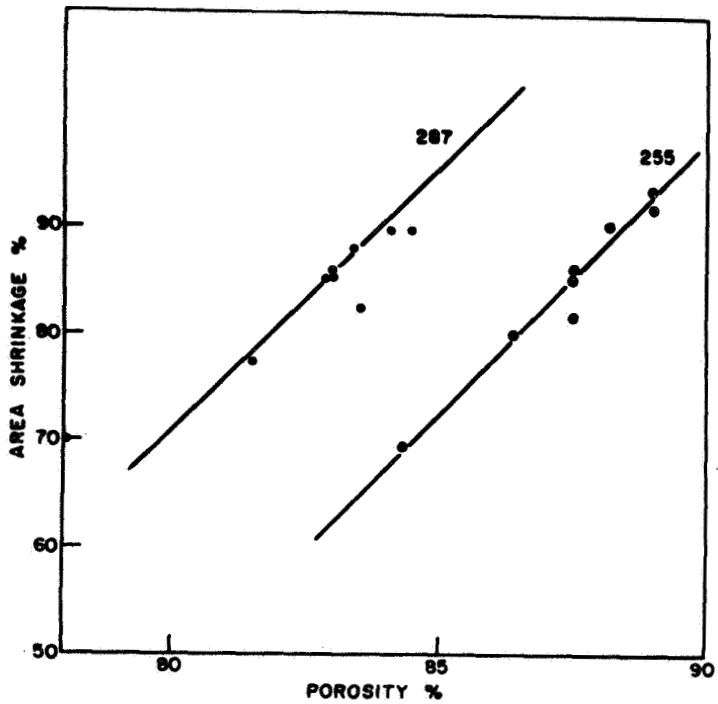

Fig. 16. Area shrinkage versus porosity

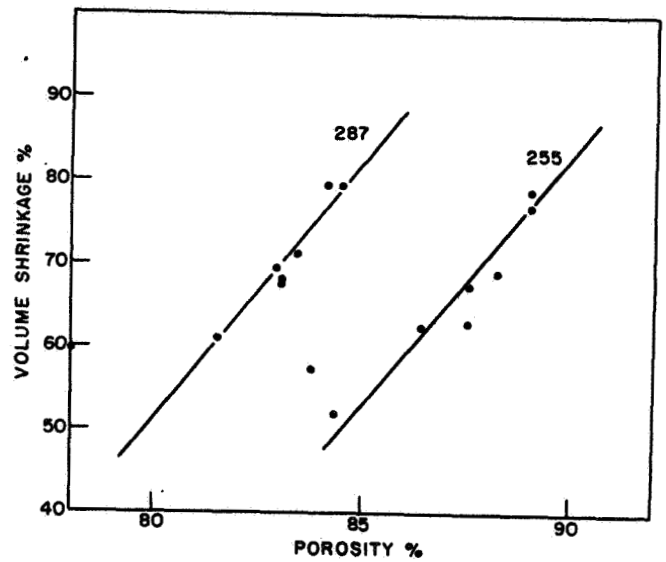

Fig. 17. Volume shrinkage versus porosity

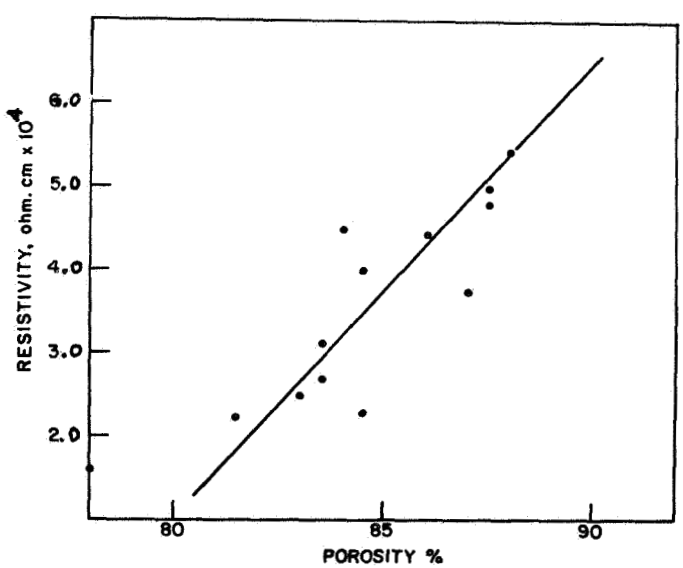

Fig. 18. Resistivity versus porosity

reduction in porosity. Since impregnated plaques still have some 45 to 50% porosity, this 5% decrease is readily tolerated. From a commercial point of view, longer sintering times and higher sintering temperatures are uneconomical, but in achieving uniformity a more highly conductive porous mass has obvious advantages.

The relationship between resistivity and surface area is presented in Fig. 19. The lower surface area that is found with the more conductive plaques is consistent with the sintering mechanism. As neck growth occurs, the surface area decreases, i. e., the total surface energy decreases. This is important from the point of view of plaque characterization in practice. Resistivity measurements are less sensitive in the presence of the conductive screen used in battery electrodes, so that plaque characterization by resistivity would be difficult. However, surface area measurements may be made using gas permeability techniques without any problems. Gas permeability techniques are also nondestructive and may be used selectively on small areas of the electrode as a test of uniformity.

Since the mechanical strength and resistivity are inversely related (see Fig. 20), it follows that the mechanical strength and surface area can be represented by a linear function as in Fig. 21.

From the above presentation, it is clear that for the loose sintering process, no specific recommendation can be made that will result in an increase in the degree of uniformity. The approach must be to take extreme care and to eliminate as far as possible potential sources of nonuniformity. Beyond this, the only suggestions that can be made are those that will minimize the influence of intrinsic heterogeneity. On this basis, the general conclusions that can be drawn from the data obtained so far is that plaques with the highest mechanical strength and conductivity, i. e., those prepared at higher sintering temperatures and longer sintering times, offer the best possibility of high uniformity.

It is also true that the rate of change of physical properties as a function of sintering time is a lot slower at extended sintering times, so that exact definition of the sintering time is less necessary. The data presented here (e. g., the minimum in the resistivity curve), suggest that optimum conditions exist at intermediate sintering times. We intend to re-examine this

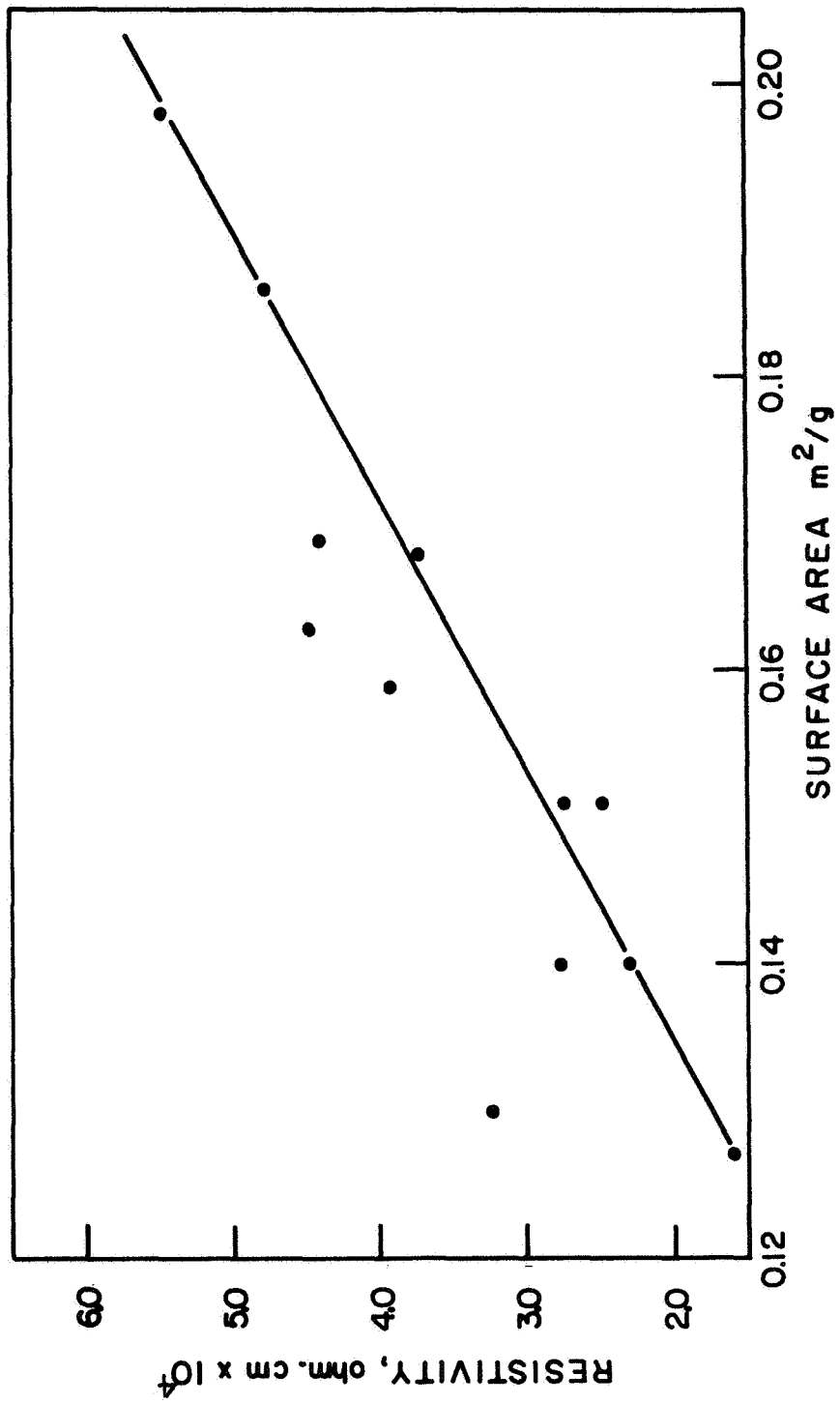

Fig. 19. Resistivity versus surface area

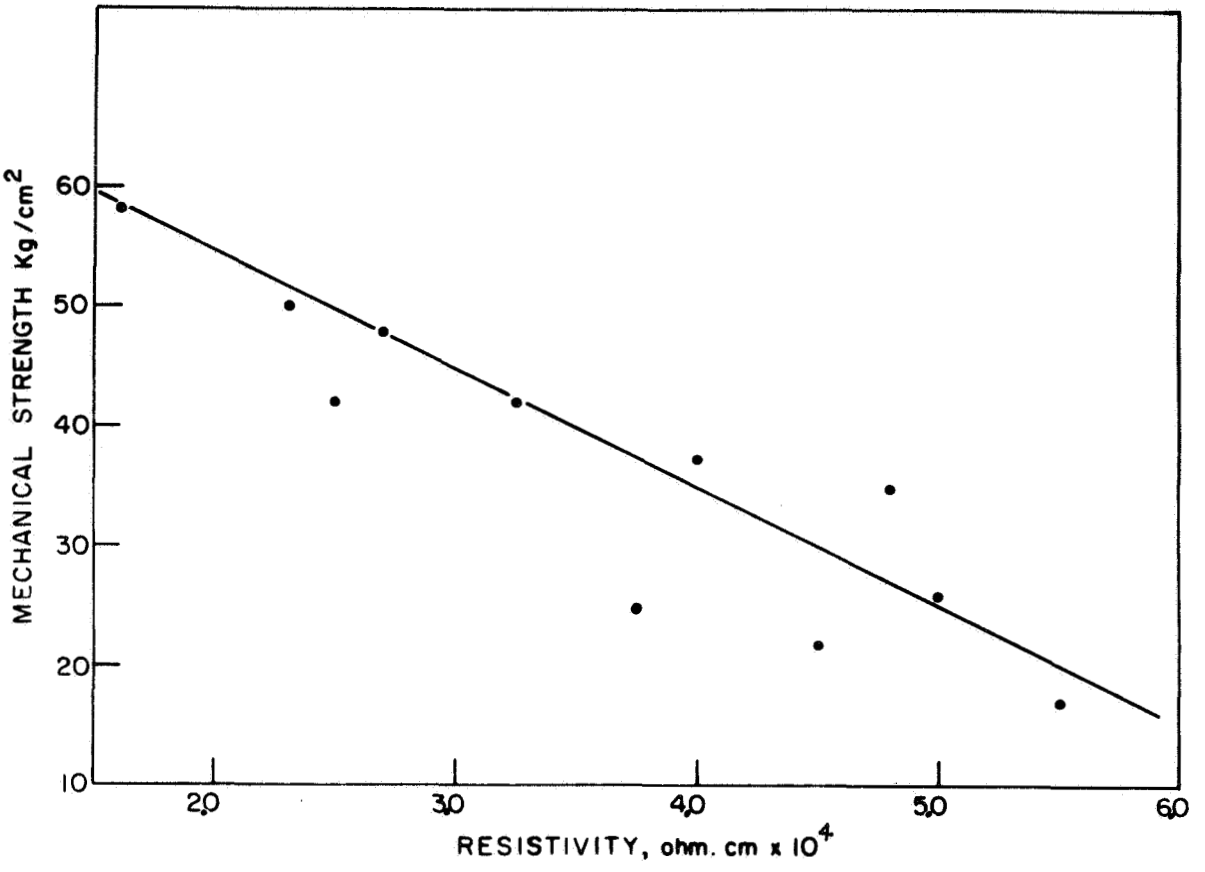

Fig. 20. Mechanical strength versus resistivity

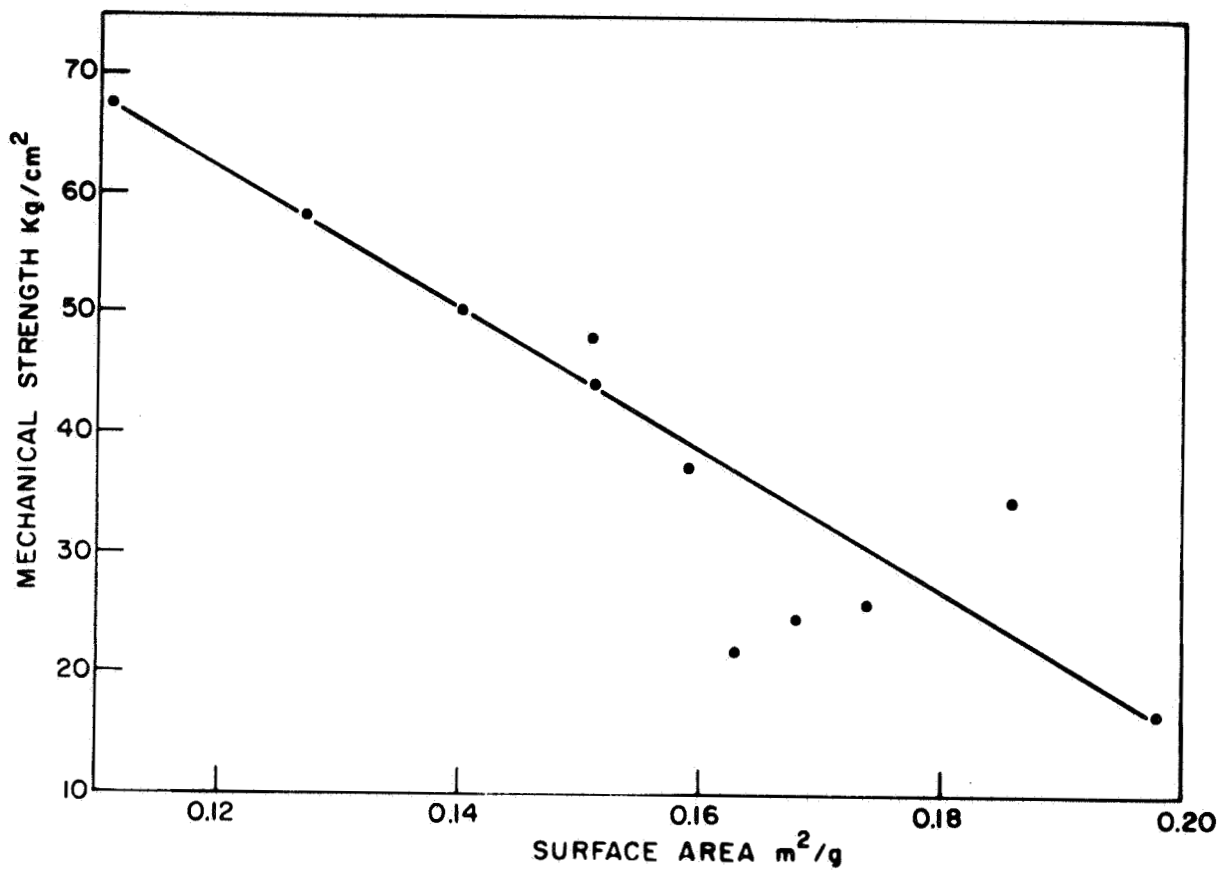

Fig. 21. Mechanical strength versus surface area

behavior to see if it is a real phenomenon or an artifact of the experimental approach. It also remains to be demonstrated that plaques prepared at longer sintering times and higher temperatures will produce plates with acceptable characteristics (i. e. , will impregnate effectively) and retain a high degree of uniformity.

A further consideration in the attempt to obtain plaques with the properties outlined above should be the rate of temperature increase in the sintering process. As discussed above, this will determine the amount of shrinkage that occurs in the powder prior to the establishment of particle to particle bonds by sintering. There is probably an optimum shape for the temperature time profile to obtain the maximum conductivity for a particular porosity figure. In the present analysis, there is little to choose between the two types of powder, since the same properties are obtained for the 255 powder as the 287 if slightly more vigorous sintering conditions are used. If plaques are compared on an equal weight basis rather than an equal volume (thickness), then there is a preference for 255. However, from a different point of view the greater filament thickness of the 287 powder will probably result in less fragmentation and thus better uniformity.

B. Measurement of Reproducibility and Uniformity

Two pairs of plaque preparations were carried out under identical conditions: LN-26 and LN-27 in a graphite mold, and LN-32 and LN-33 in a Vycor lined graphite mold. Summary tables of results were given in the previous section. In Table XVII the thicknesses, porosities, and surface areas of each of the nine pieces into which the plaques were cut are given as a function of position.

In the case of LN-26 and LN-27, there are no gross inconsistencies; the average thickness proved to be quite reproducible (0. 0241 and 0. 0239 in. , respectively). There are, however, variations across the plaque ranging from 0. 0228 to 0. 0247 in. , but the trends for both plaques are the same reflecting the method of leveling. The leveling process involved drawing a striker blade from the ABC edge in a zig-zag pattern across the mold as discussed earlier in this report. This resulted in a thicker plaque towards the end of the drawing stroke, and also increased thickness towards the edges.

Table XVII. Physical Properties as a Function of Position

	LN-26			LN-27		
Porosity, %	82.7	82.1	82.5	82.7	83.4	84.1
	83.1	82.8	82.5	82.6	82.6	83.3
	83.2	85.4	83.3	82.2	83.1	83.5
Mean			83.4			83.2
Thickness,	0.0243	0.0228	0.0241	0.0237	0.0227	0.0240
in.	0.0244	0.0238	0.0240	0.0238	0.0235	0.0245
	0.0247	0.0242	0.0246	0.0246	0.0241	0.0245
Mean			0.0241			0.0239
Surface Area,	0.147	0.122	0.150	0.144	0.119	0.152
m^2/g	0.145	0.157	0.145	0.152	0.132	0.142
	0.156	0.141	0.131	0.141	0.147	0.135
Mean			0.144			0.140
Surface Area,	0.227	0.194	0.234	0.222	0.176	0.215
m^2/cm^3	0.218	0.240	0.226	0.238	0.204	0.211
	0.233	0.198	0.194	0.223	0.221	0.198
Mean			0.217			0.212

The average porosities showed very good agreement (83.4% and 83.2%, respectively, for LN-26 and LN-27). The porosity was also much more uniform than the thickness, all the values falling within a 3% spread.

The surface area in m^2/g showed larger variations, though again the mean values for the two plaques (0.140 and 0.144 m^2/g) are in good agreement. The spread in values is ~20% of the mean value; the reproducibility of the method of measurement has been shown to be $\pm$ 3%. Measurements of surface area would appear to be a sensitive method of determining nonuniformity.

We may also calculate the surface area per unit volume of the plaque. This figure eliminates the variations due to porosity and thickness inherent in the m^2/g figure, since it represents a direct measure of the internal surface morphology of various regions of the plaque (this factor is probably important in the impregnation process). Since these figures show little improvement in uniformity, we must assume that the mold filling and leveling processes have a direct effect on the characteristics of the plaque beyond those of porosity and thickness. For example, the differences in the amount of compaction introduced inadvertently during the leveling would (1) increase the number of particle to particle contacts, (2) locally increase the neck growth, and thus reduce surface area. The measurement of porosity is not sufficiently sensitive to reflect these differences. Differences are, however, evident in the direct measurement of resistivity and mechanical strength which show considerable variation.

The principal conclusions are therefore that loose sintering is not an acceptable method for preparing uniform plaque material, and that the measurement of porosity is a relatively insensitive method of detecting nonuniformity.

An examination of the data for plaques LN-32 and LN-33 confirms these conclusions, though for these plaques the reproducibility is not as good and there is more spread in the uniformity tests. This is attributed to the use of a blended powder and depends on factors that will be discussed in detail below.

C. Influence of Powder Properties on Plaque Characteristics

As discussed previously, it was considered that the blending of two types of carbonyl nickel powders to give progressive changes in powder characteristics would give more valuable information on the control of plaque characteristics than a study of a range of nickel powders prepared by different methods. It is also standard commercial practice to blend powder batches to obtain a specified bulk density for the operation of the slurry coating process for plaque fabrication. The data gathered here are therefore more relevant to practical problems.

The specific objectives of this aspect of the work were: (1) to assess the effectiveness of blending, (2) to examine the associated variations in the powder properties other than bulk density and their influence on plaque characteristics, and (3) to define the effect of blending on plaque uniformity. The blended powders consisted of the following: M-1, 20% 255, 80% 287; M-2, 40% 255, 60% 287; M-3, 60% 255, 40% 287; M-4, 80% 255, 20% 287. Also included in the analysis are the individual components of the mixture M-0, 100% 287, and M-5, 100% 255. The bulk densities of these materials are presented in Fig. 22. The figures for the blended mixtures all lie above a linear interpolation of the bulk densities of the components, with the extent of the difference increasing with the content of 255, i.e., as the actual bulk density figure decreases. If, instead of the bulk densities measured for the components, we take the mean value of the numerous measurements made during the determination of the sampling and experimental errors in the early part of this program, then a reasonably linear plot is obtained. It is significant that for the sampling measurements the powders were carefully blended by exactly the same techniques used with the above mixtures. Blending, even when carefully carried out in a gentle manner, has the effect of increasing the bulk density. This increase is due to the breaking of the filament-like structures of the powders, and it would seem that the filaments of the 255 powder are more prone to fracture than those of 287.

The surface areas of these powders are plotted in Fig. 23. There is considerable scatter in the points indicating that the blending process

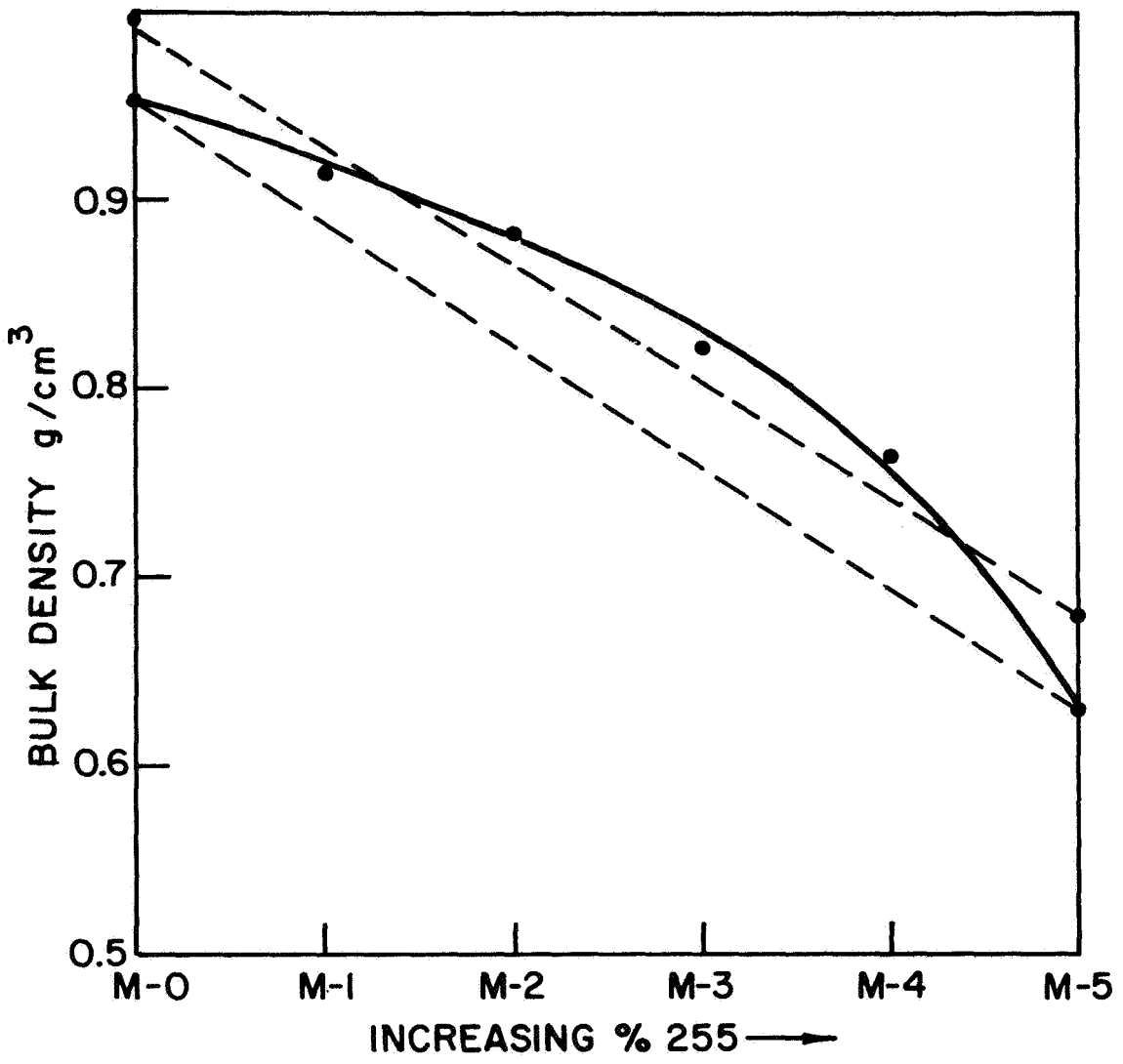

Fig. 22. Bulk density of blended powders

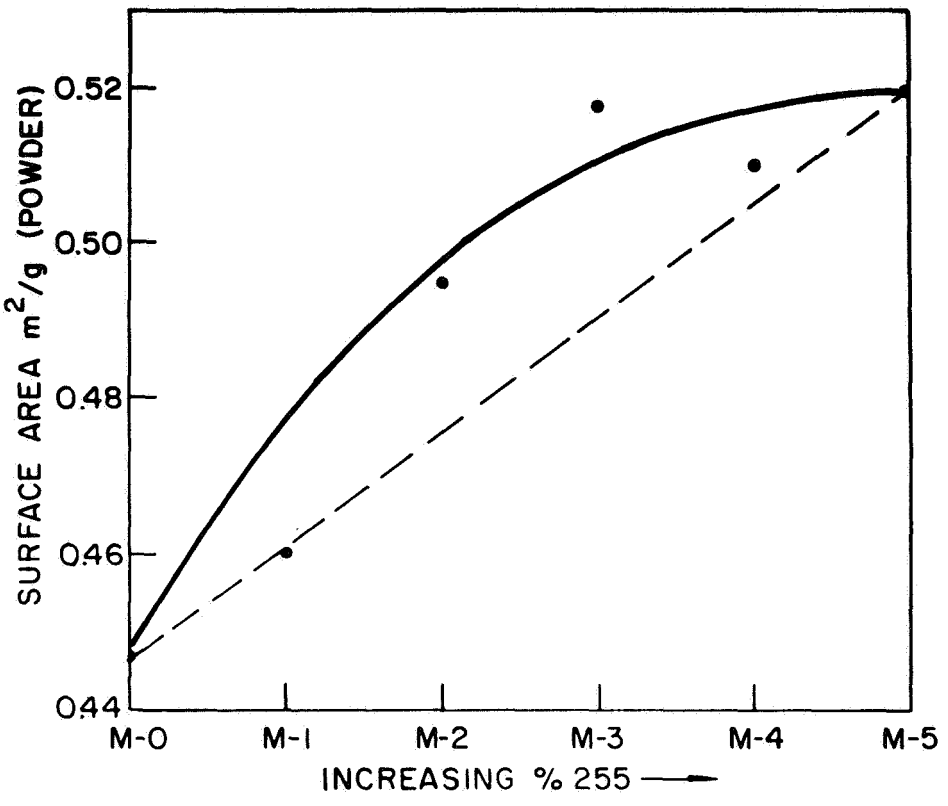

Fig. 23. Surface area of blended powders

produces random rather than consistent changes in powder properties (the time and method of blending were identical in each case). The surface area increases rapidly with increase in percentage 255 up to 60%, after which the values level off. This effect is apparent in Fig. 24, a plot of surface area against bulk density. It is important to note that very large changes occur in surface area for only small changes in bulk density, i.e., the characteristics of the powder is altered significantly.

The change in Fisher number with percentage 255 is shown in Fig. 25. Here the change is reasonably progressive. Plotted as a function of bulk density, the Fisher number increases rapidly with increasing 255 content initially and then levels off as does the surface area. The fact that these plots do not show as much scatter as the surface area plots* is not too surprising. The Fisher number for filamentary powders will be primarily determined by filament diameter and will not be very sensitive to the additional surface area produced by filament fracture. This additional area would, of course, contribute to the BET determination of surface area (note that all the BET areas are larger than the linear interpolation). As shown in Fig. 26, the variation of Fisher number with bulk density does show a somewhat different trend.

A plot of Fisher number against BET surface area should give a unique straight line if the assumptions implicit in the Fisher determination are justified. It is interesting to note in Fig. 27 that two well defined linear regions are obtained.

The average crystallite size determined by X-ray line broadening plotted as a function of percentage 255 in Fig. 28 also shows widely scattered points, emphasizing the inefficiency of the blending process. (There is no reason why crystallite size should change with blending.)

For the general survey of plaque properties, three measurements of each variable were made on sections B, E, and H as described earlier and presented in Table XI. The more comprehensive analysis of the M-2 plaques

*The Fisher number is an equivalent uniform spherical diameter based on a surface area determined from air permeability measurements.

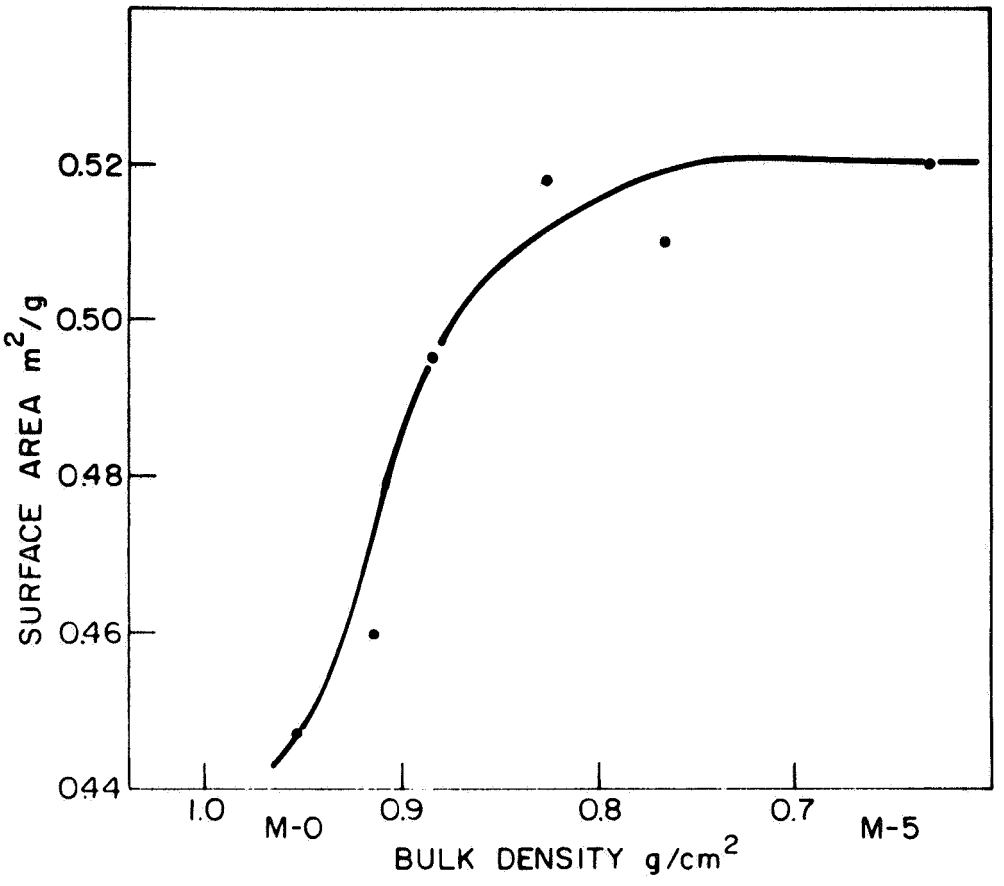

Fig. 24. Surface area of blended powders versus bulk density

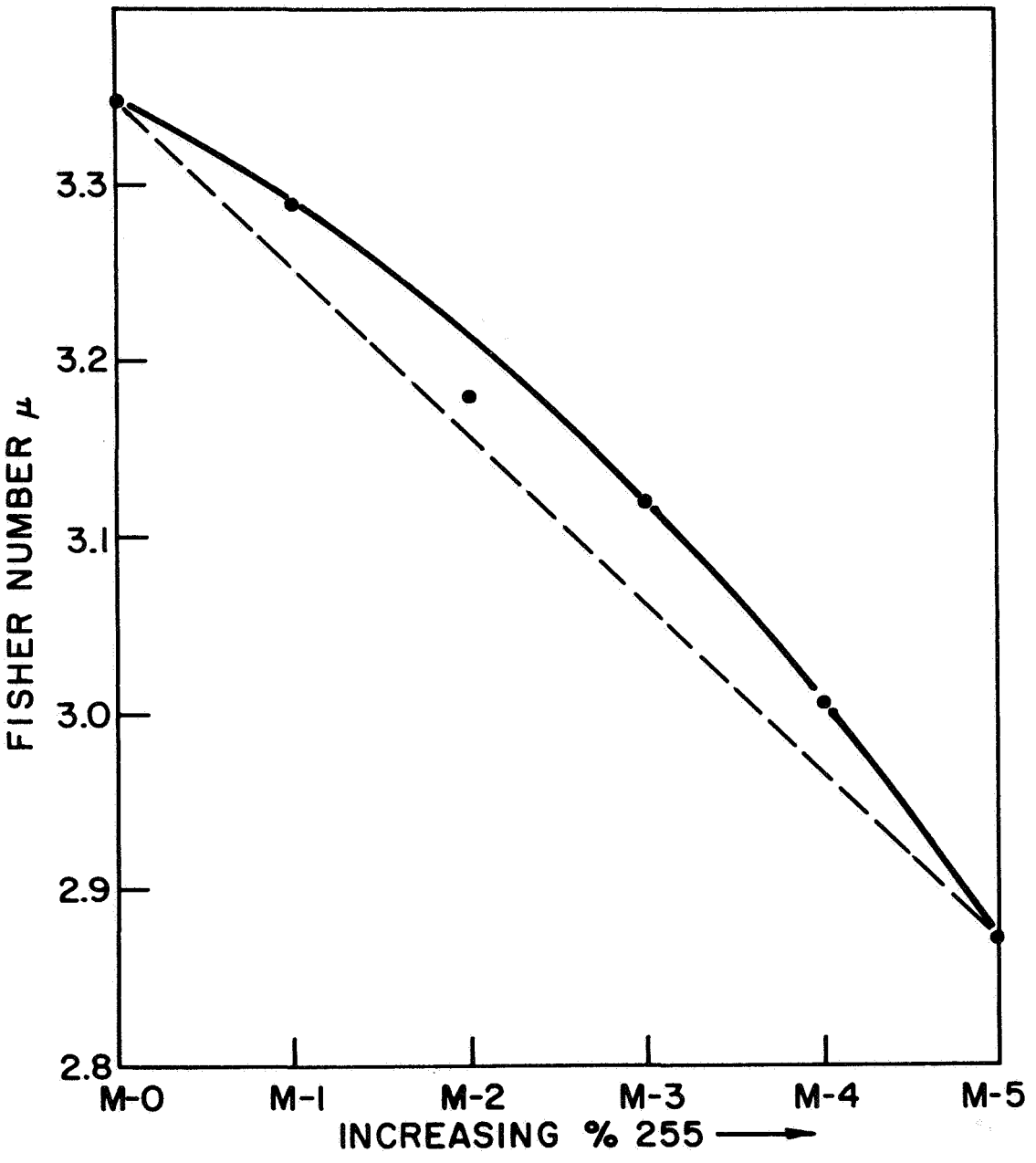

Fig. 25. Fisher number of blended powders

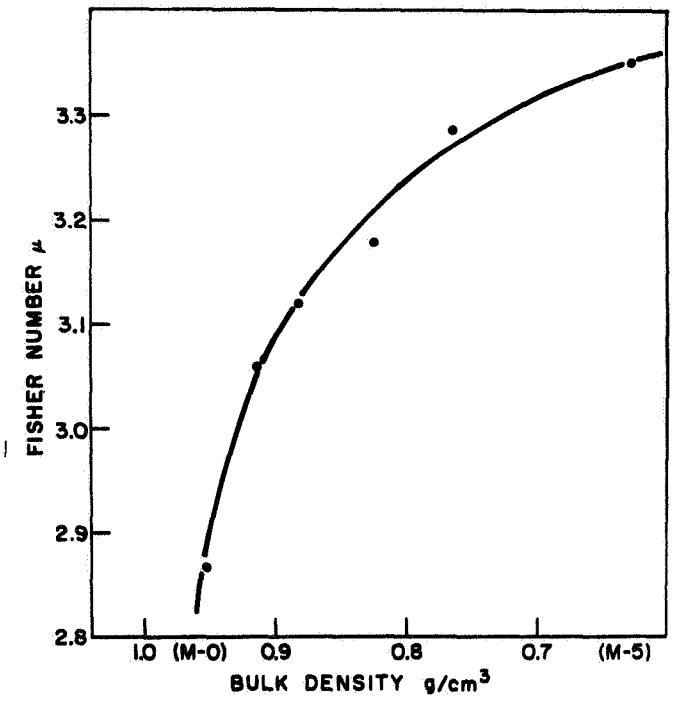

Fig. 26. Fisher number of blended powders versus bulk density

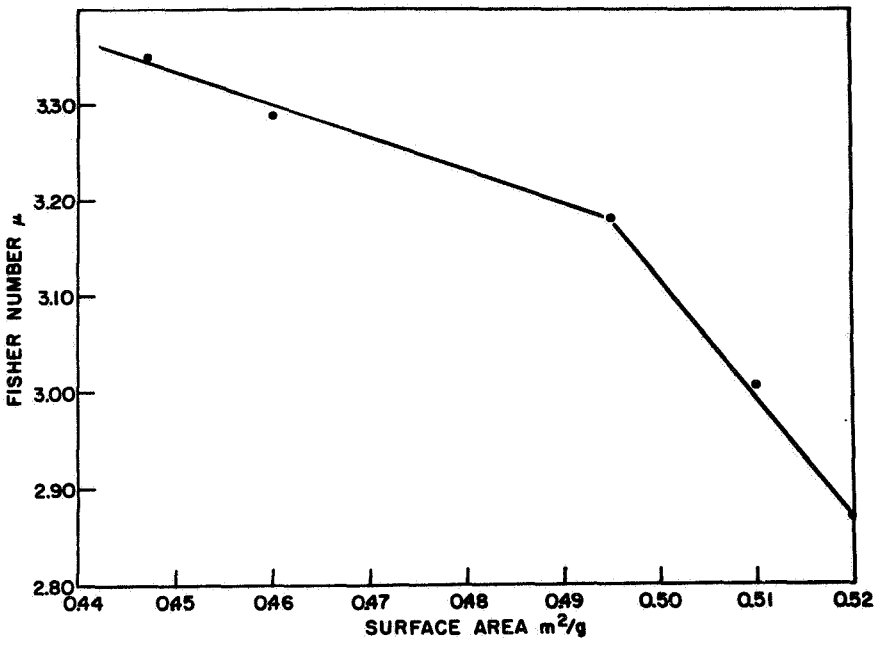

Fig. 27. Fisher number of blended powders versus surface area

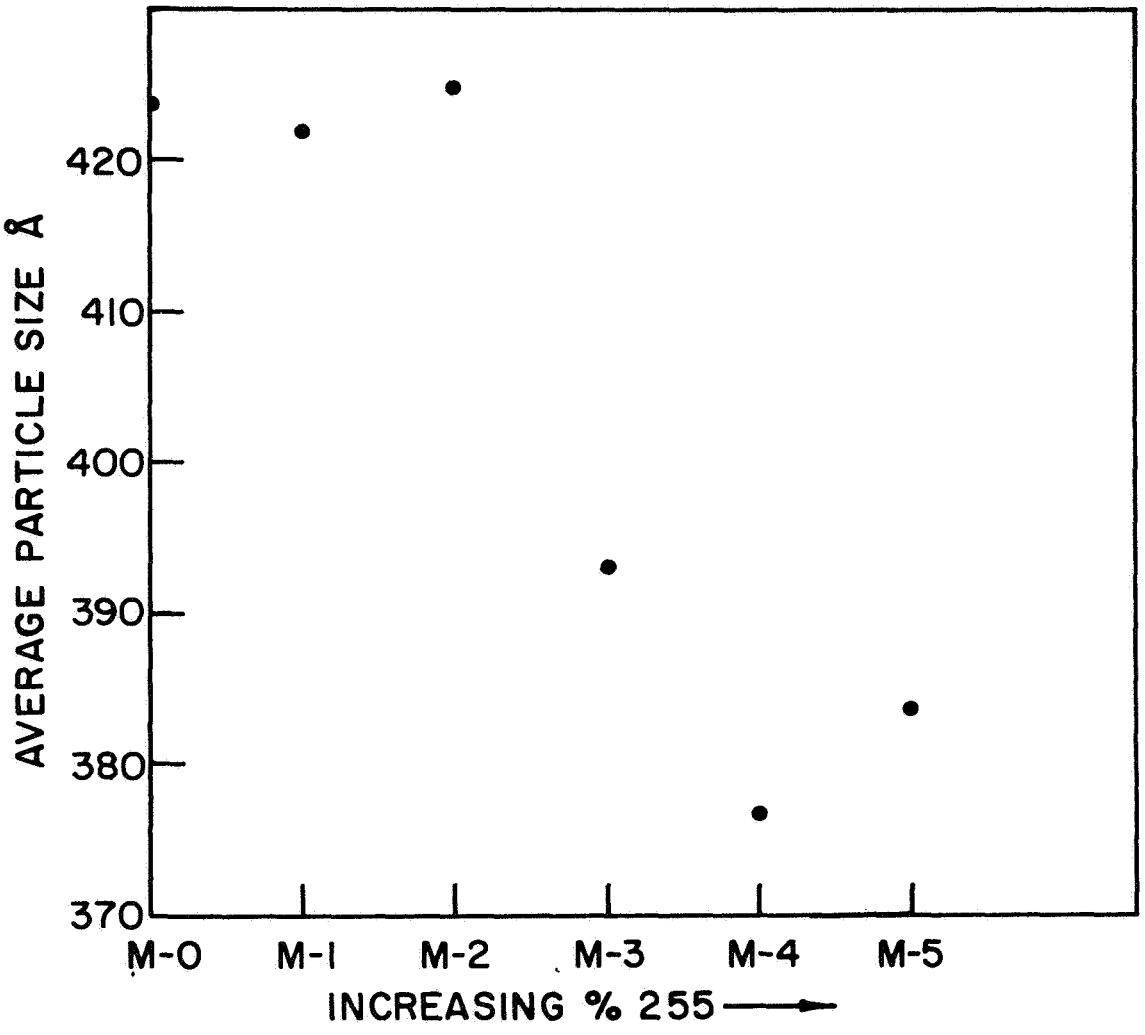

Fig. 28. Average crystallite size of blended powders

was described in the previous section. Since, throughout these analyses the results for M-1 are inconsistent, the general conclusions presented below disregard the M-1 values.

Fig. 29 shows the variation in porosity with the 255 content of the powder; a steady increase in porosity is observed as would be expected.

The surface area plot in Fig. 30 shows considerable scatter, again indicating the sensitivity of this measurement in identifying nonuniformity.

The resistivity measurements (Fig. 31) display unusual behavior in that the addition of 20% 287 to the 255 powder produces a considerable increase in conductivity, but further additions apparently have little effect. Surprisingly, this pattern is not reproduced in the mechanical strength measurements in Fig. 32.

In Figs. 33 to 36, the same plaque properties considered above are presented as a function of the bulk density of the powder. As would be expected, the porosity plot is approximately linear. Due to the large scatter in the surface area values, the line drawn can only be considered as indicative of the trend of surface area change with bulk density. The resistivity and mechanical strength plots are very similar to those of Figs. 31 and 32.

The correlations between resistivity and surface area, and mechanical strength and surface area presented in Figs. 37 and 38 do not show the consistency of the data presented in Figs. 19 and 20 for the unblended powders. This difference must be ascribed to the nonuniformity of the blending process. The interrelation of mechanical strength and resistivity is emphasized by the points plotted in Fig. 39.

The pore size distribution in the plaques is given in Fig. 40. A more detailed interpretation of the shape of these curves is given below. At this stage we may note that the total penetration volumes agree very well with the porosities calculated from the weight and dimensions of the plaques, e. g., the penetration volume for M-5 corresponds to 89% porosity and for M-0, 82.5%. The pore size distributions do not appear to be significantly different but, as will be discussed below, the very rapid increases in penetration volume between 12 and 17 μ do not, as is commonly assumed, represent a very narrow pore size distribution.

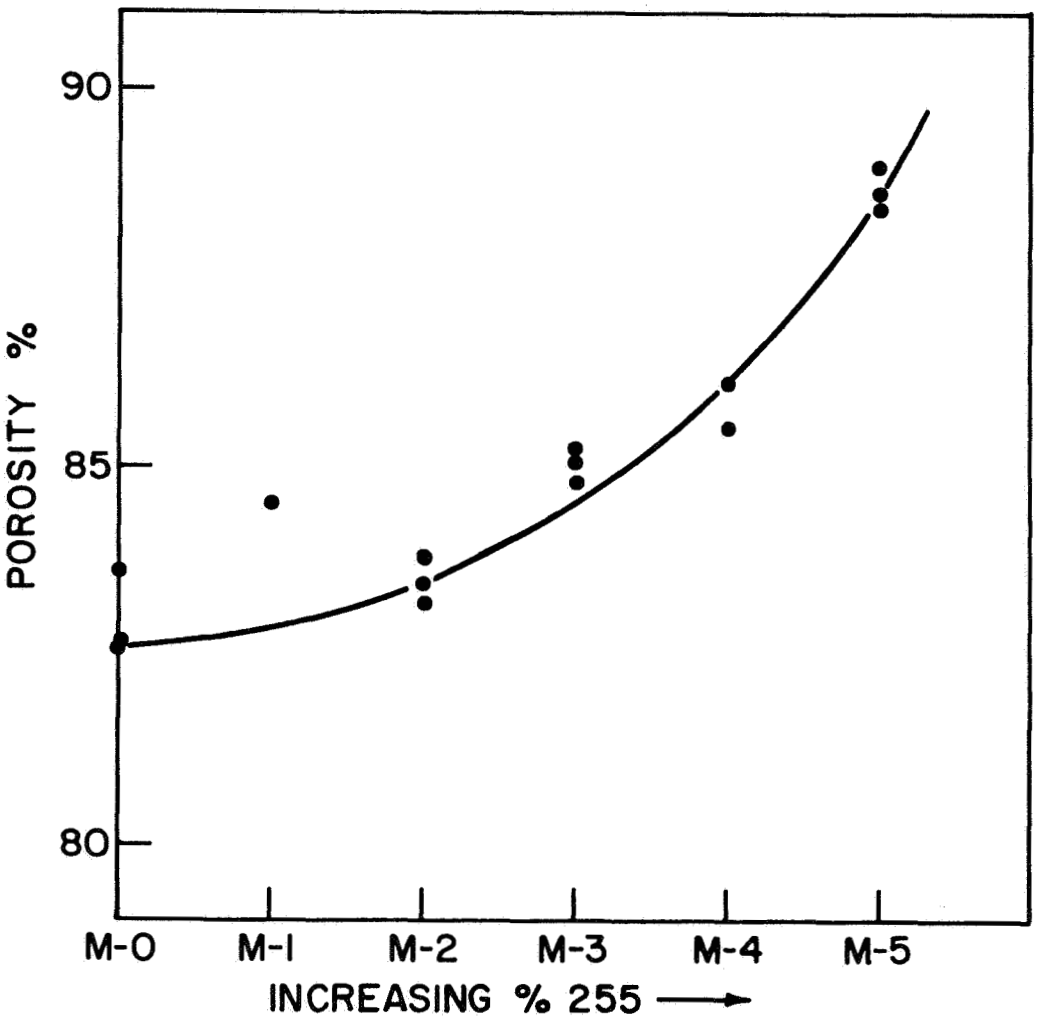

Fig. 29. Porosity of plaques prepared from blended powders

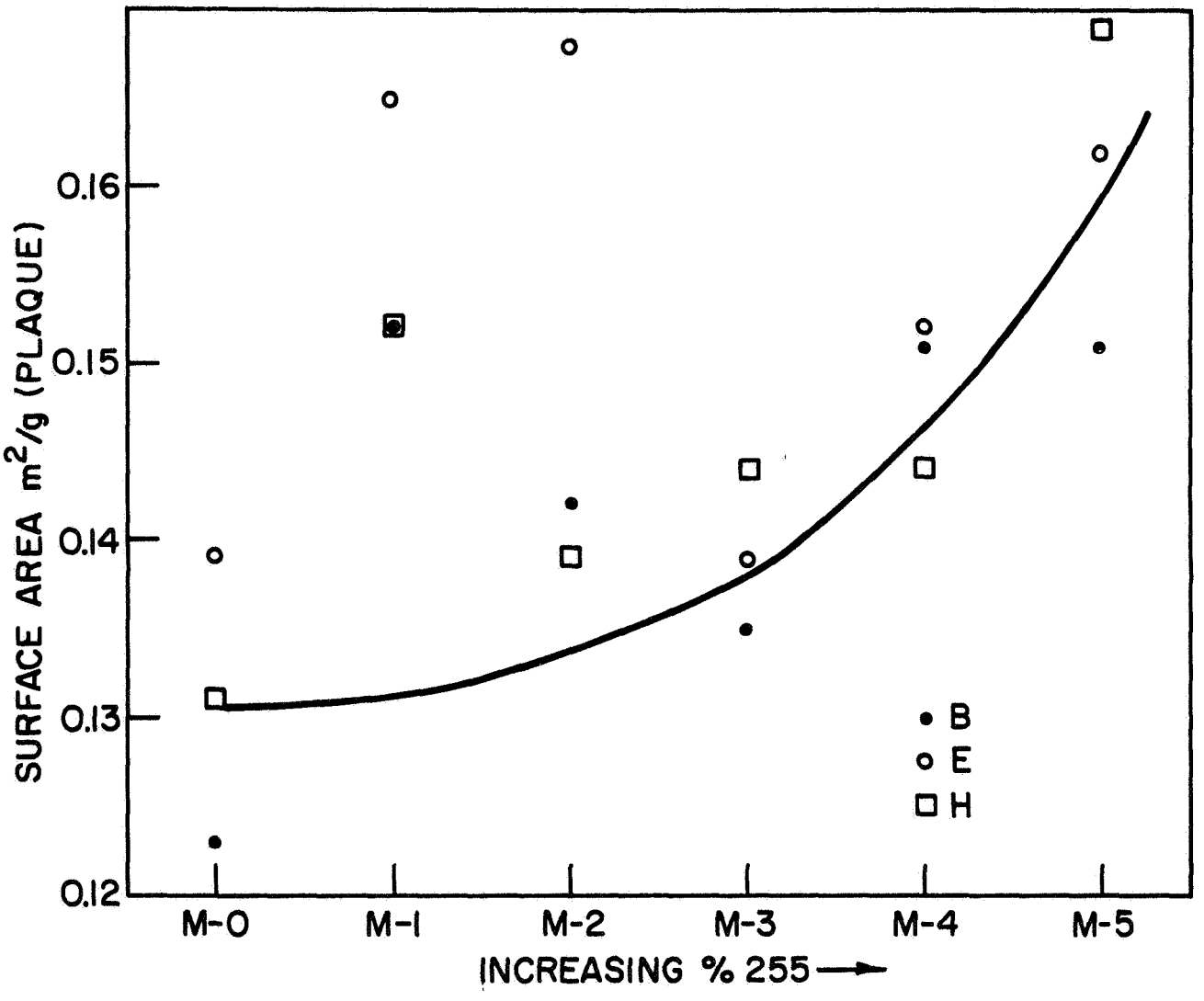

Fig. 30. Surface area of plaques prepared from blended powders

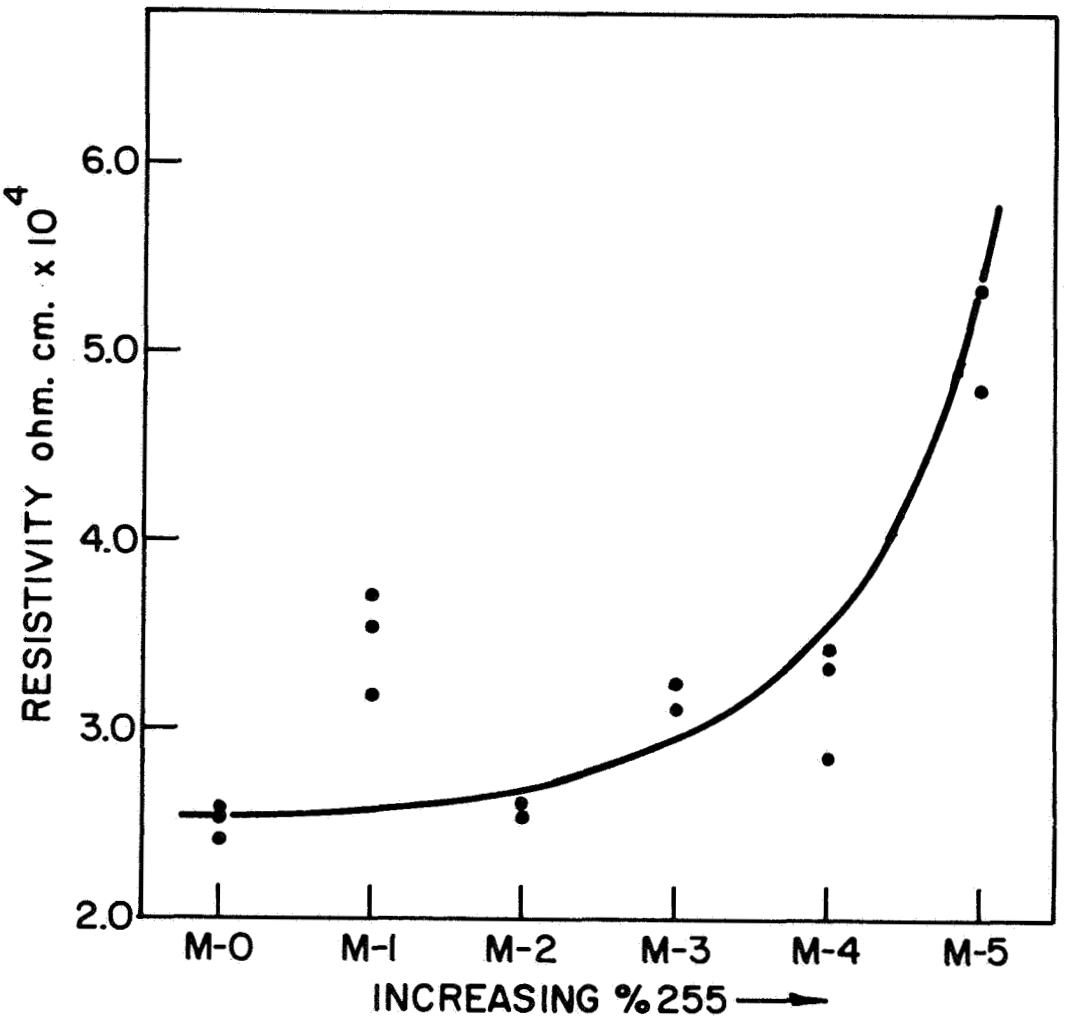

Fig. 31. Resistivity of plaques prepared from blended powders

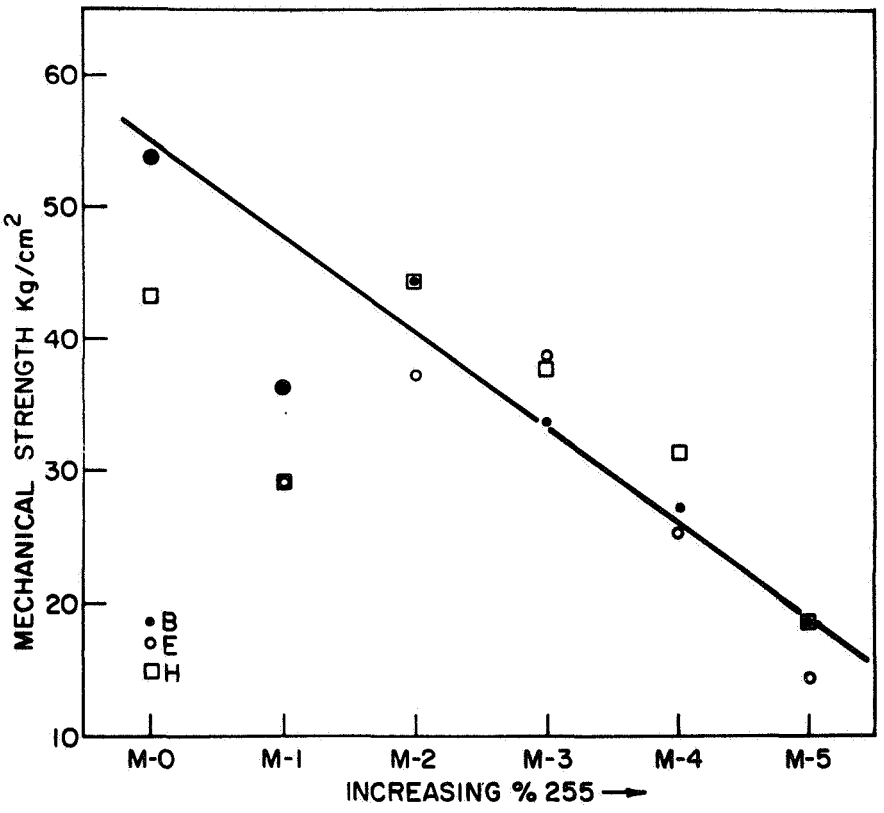

Fig. 32. Mechanical strength of plaques prepared from blended powders

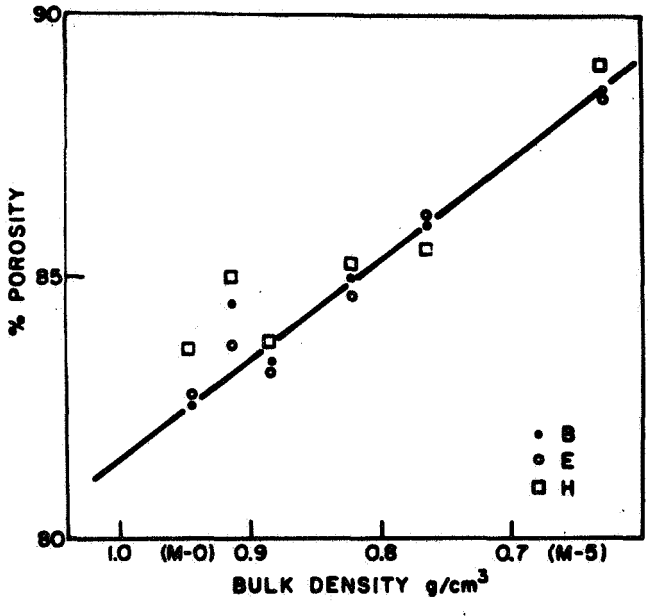

Fig. 33. Porosity versus bulk density of blended powders

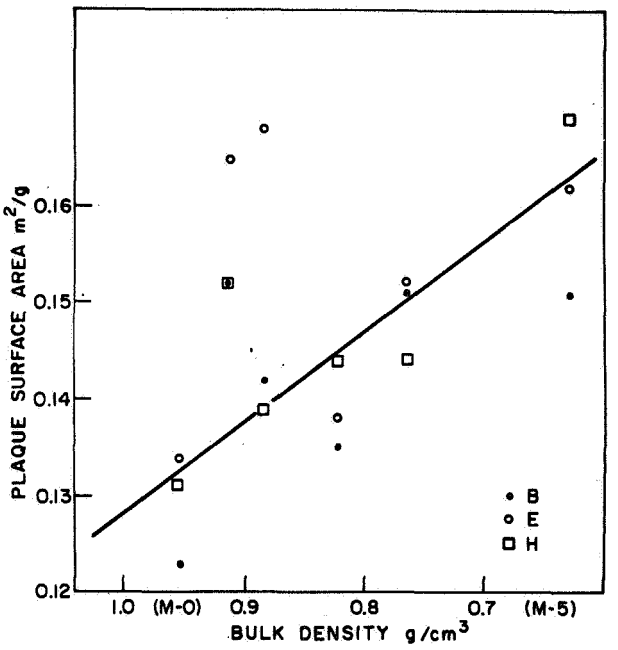

Fig. 34. Plaque surface area versus bulk density for blended powders

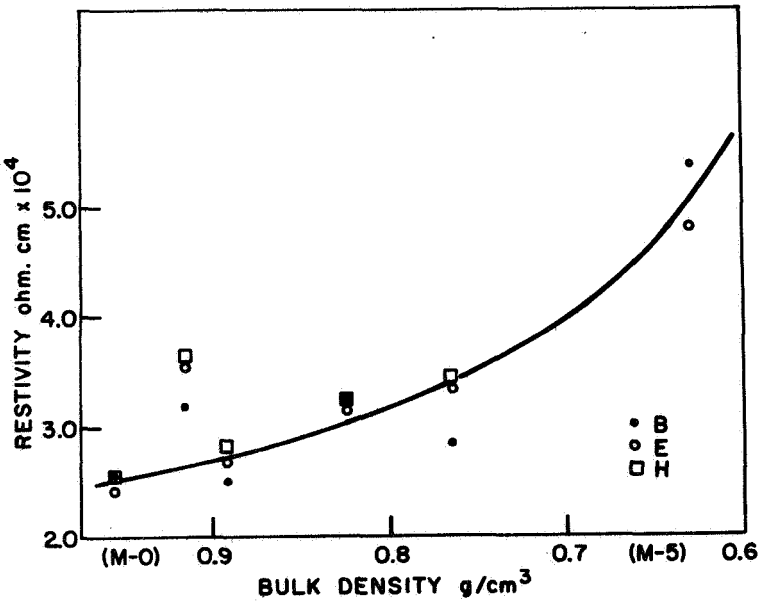

Fig. 35. Resistivity versus bulk density of blended powders

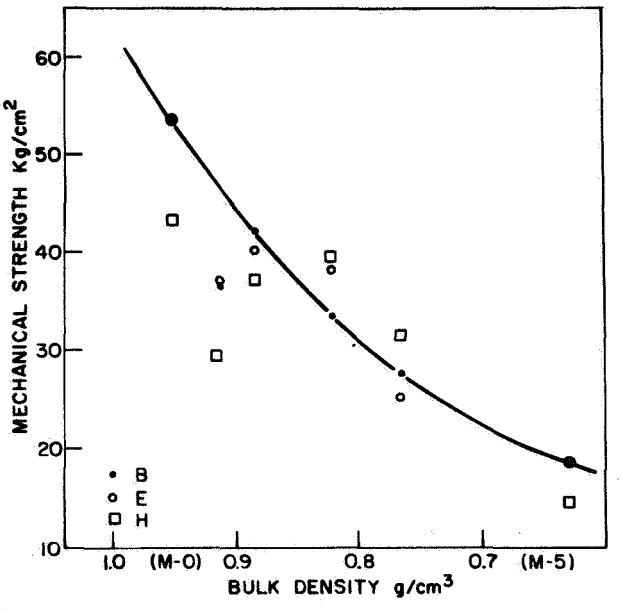

Fig. 36. Mechanical strength versus bulk density of blended powders

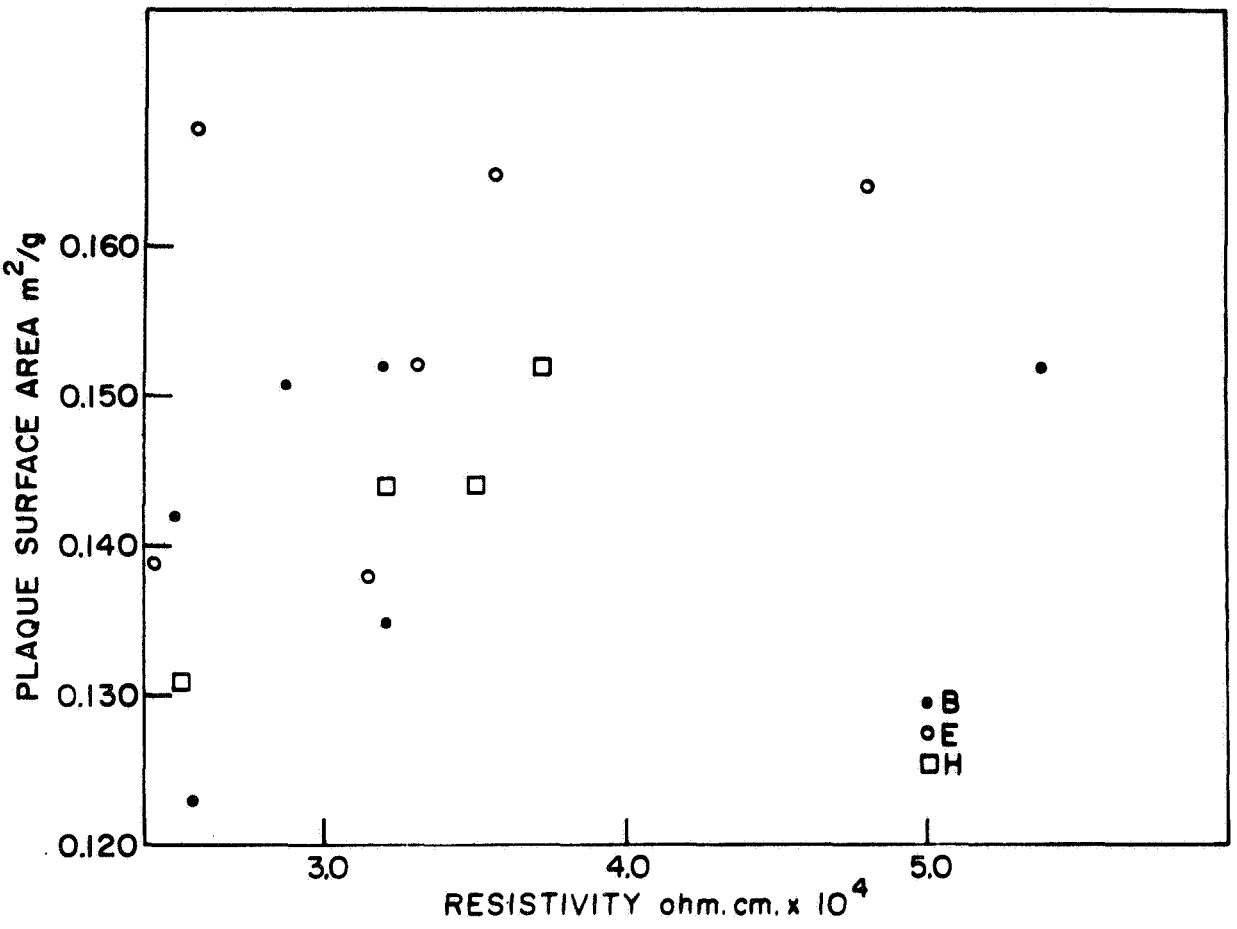

Fig. 37. Plaque surface area versus resistivity

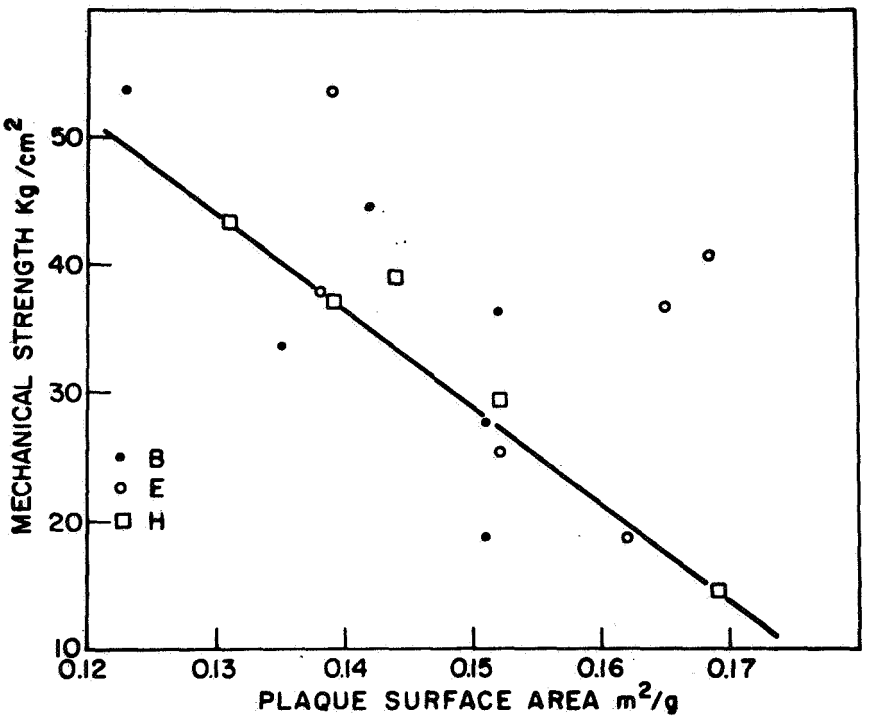

Fig. 38. Mechanical strength versus plaque surface area

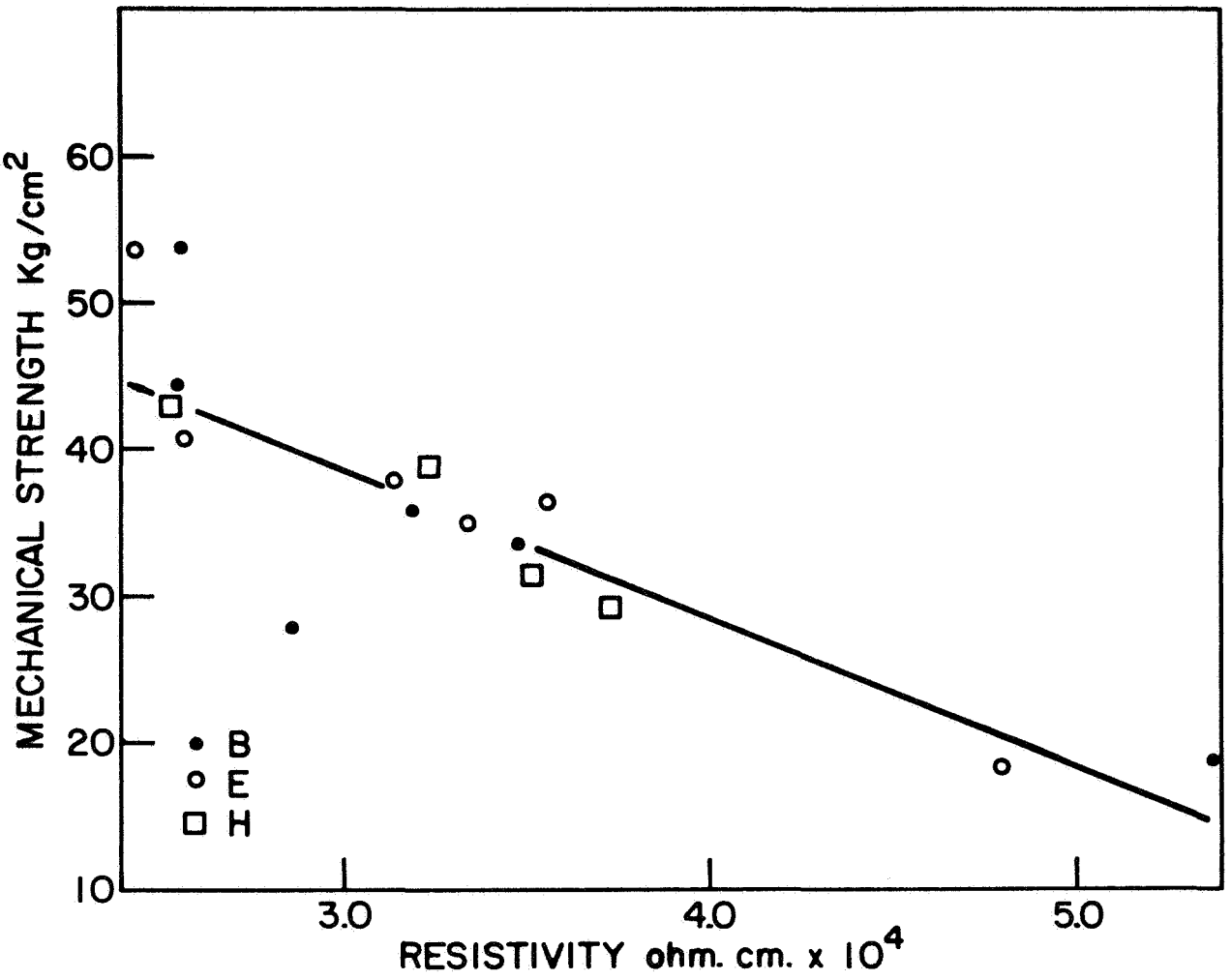

Fig. 39. Mechanical strength versus resistivity

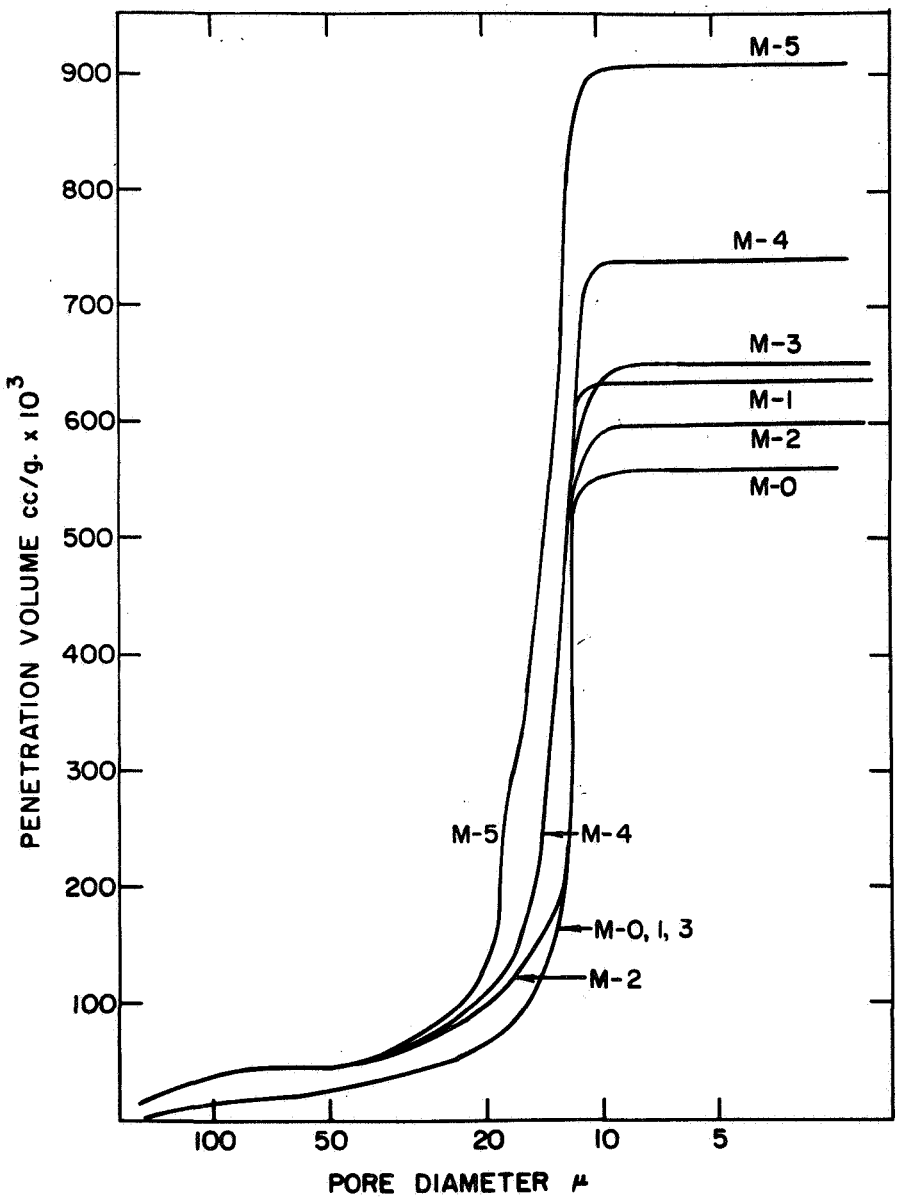

Fig. 40. Pore size distribution in plaques from blended powders

In summary, the principal conclusion to be drawn from the above data is that efficient blending of these powders is difficult. Even under the mild conditions in our experiments, the physical characteristics of the powders were significantly changed. More vigorous mixing would certainly destroy to a large extent the important properties of these powders. For example, there would be an effective loss in porosity before the sintering process was even begun.

Thus, unless the commercial methods of mixing are substantially more efficient, blending will be a serious source of poor reproducibility and nonuniformity in the physical properties of the starting material, properties that are undoubtedly reflected in the quality of the plaque.

D. Interpretation of Porosimetry Measurements

Data presented in the Second Quarterly Report showed a discrepancy between mean pore sizes defined by mercury porosimetry and those obtained by quantitative metallography. The metallographic figures are summarized in Table XVIII. These are substantially larger than the 7 to 8 μ obtained for these plaques by mercury porosimetry.

It is considered that the discrepancy is due to the assumption of a cylindrical pore model in calculating pore size data and, further, to the interpretation of the very sharp rise in the penetration volume versus pressure curve as a very narrow range of pore size. The highly porous electrode structure shown in the scanning electron micrographs in Figs. 41 and 42 (reproduced from Goddard Special Document X735-68-400), is better considered as a skeleton structure of solid cylindrical filaments of nickel randomly oriented in space.

For the purpose of further discussion, however, it is more convenient to examine the behavior of the porous mass as a lattice of very open parallel grids of uniform dimensions. In mercury penetration experiments, we can then envisage that the first process will be the formation of mercury "drops" inside the porous structure. This is demonstrated in Fig. 43 which represents a section through two filaments in the surface of the porous mass forming two sides of a pore, and two parallel filaments below the surface. With no excess

Table XVIII. Quantitative Metallography

Plaque No.	Powder Type	Sintering Conditions		Average Porosity, %	Metallographic Porosity, %	Average Pore Diameter, μ
		Time, min	Temperature, °C			
LN-1	255	30	820	86	85.9	19.2
LN-2	255	20	822	87	72.3	17.3
LN-3	255	10	817	89	86.5	22.0
LN-4	255	5	805	80	88.4	19.6
LN-5	255	30	728	90	87.0	18.3
LN-6	255	20	720	90	79.6	21.2
LN-7	255	10	700	88	89.0	22.5
LN-8	255	5	673	90	86.0	22.1

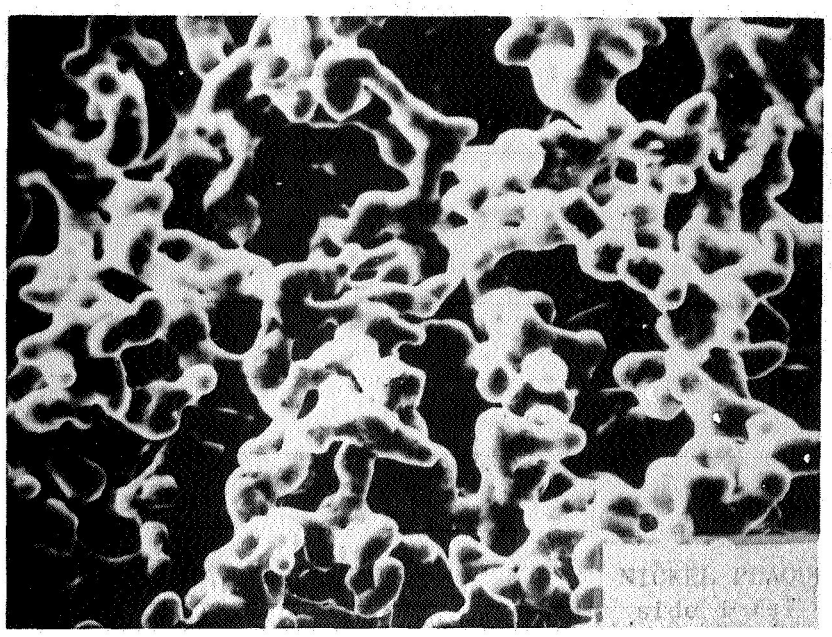

Fig. 41. Scanning electron micrograph of nickel plaque ~ 1500 X

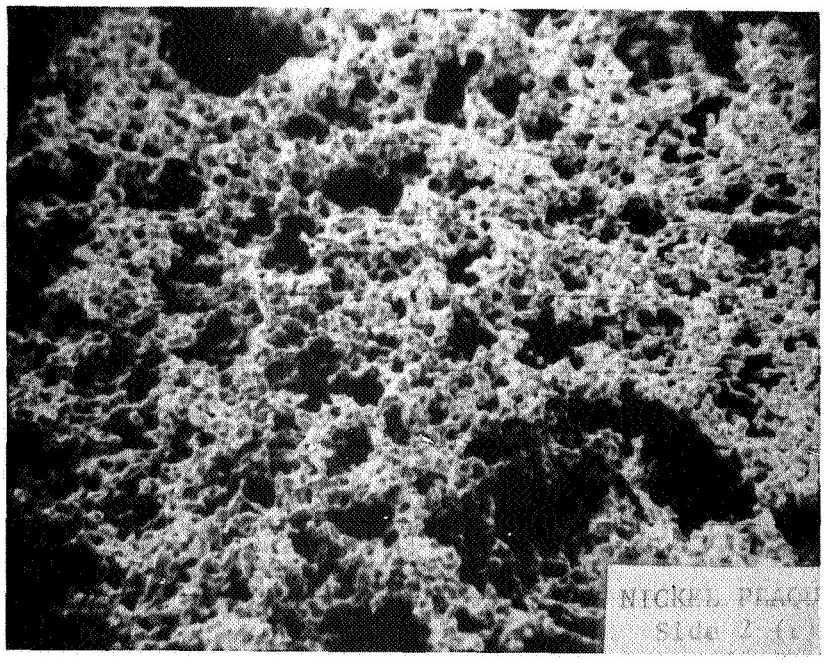

Fig. 42. Scanning electron micrograph of nickel plaque ~ 300 X

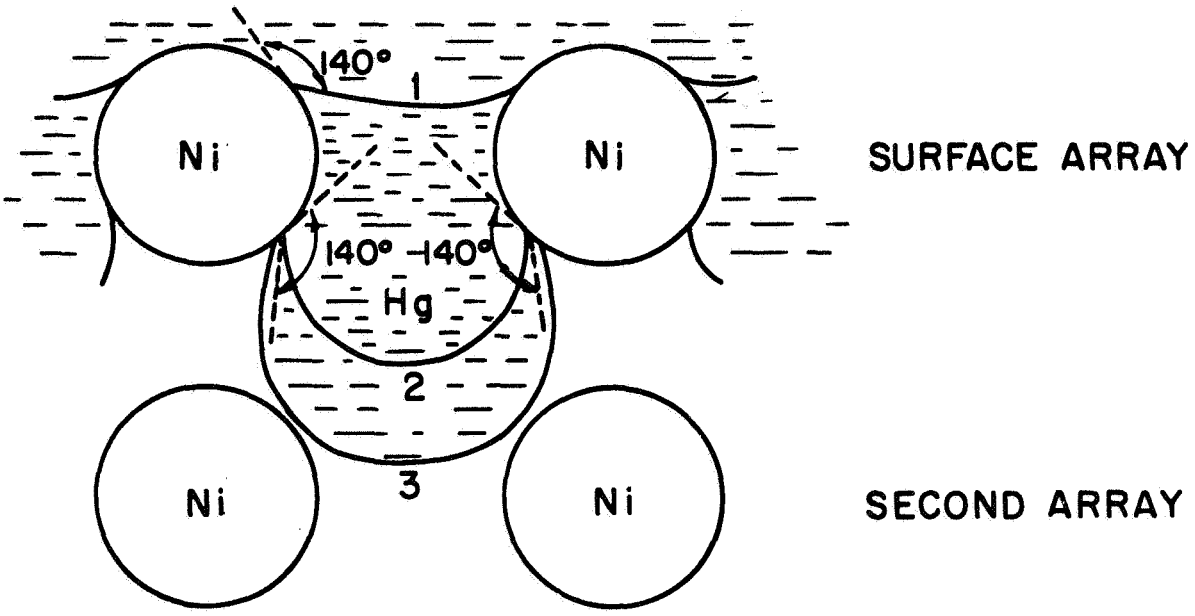

Fig. 43. Mercury penetration of highly porous nickel plaque

pressure, the meniscus would take up a shape similar to that shown as position 1, with the mercury-filament contact angle of the order of ~140°. As the pressure on the mercury is increased, a mercury drop will form as indicated by position 2 (still maintaining a contact angle of ~140°). When, however, the pressure reaches the point where the drop has grown to touch the filaments below the surface (position 3), the surface energy of the drop is lost and mercury floods into the structure to fill it completely. In effect, drop formation and destruction now occur at each layer in the porous mass progressively and in a very rapid fashion. This breakthrough pressure results in the very rapid increase observed in the penetration volume versus pressure curves referred to earlier and shown in Fig. 40. Note that the drop formation is relatively insensitive to pore size. In most cases, the larger pores will be associated with larger void spaces between the surface and subsequent layers, so that large drops will grow from the large pores and small ones from the small pores. Both structures will have approximately the same breakthrough pressure. It should also be recognized that the volume of mercury associated with drop formation is small compared to the total internal volume of the porous mass.

This concept is supported by the hysteresis phenomena that are observed in mercury penetration experiments with nickel battery plaques. A typical example is shown in Fig. 44. In region 1, that corresponding to drop formation, the penetration behavior is completely reversible and the curve may be traced in either direction to give identical penetration volumes. If, however, the breakthrough pressure is exceeded, then considerable hysteresis is observed. By careful experimentation in the vicinity of the breakthrough pressure, region 2 can be traced quite precisely. The shape of this region of the curve is very similar to that which is observed if the complete pressure range is retraced.

We must then conclude that the effective pore size lies in the range defined by region 1 of the curve presented in Fig. 44, i.e., in terms of cylindrical diameters from 8 to >30 μ. These values correspond to those observed in the quantitative metallography. The apparent pore diameter normally associated with the breakthrough pressure is probably more significant if it is considered as a structural parameter of the plaque.

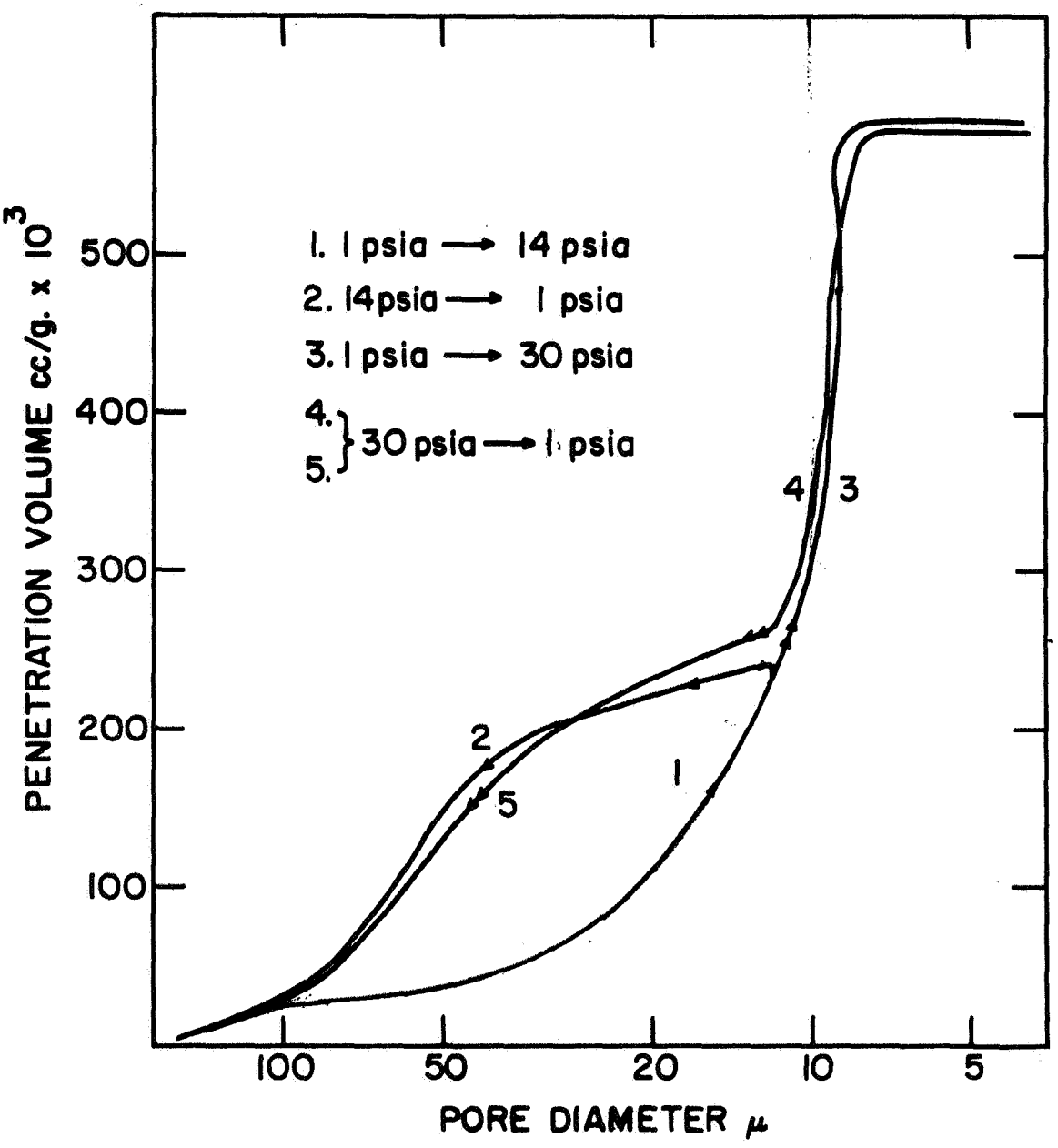

Fig. 44. Hysteresis in penetration volume

It should be noted that this wide distribution of pore sizes does not conflict with an objective of uniformity. As long as the shape of the distribution from plaque to plaque and from point to point within a plaque does not change markedly, the plaques meet our uniformity and reproducibility criteria. The distribution could, however, be far from optimal from the point of view of utilization of active material and, in the presence of other sources of nonuniformity, could result in detrimental practical effects that might otherwise have been avoided.